

Minimizing Eigenvalues for Inhomogeneous Rods and Plates

Weitao Chen¹ · Ching-Shan Chou² · Chiu-Yen Kao³

Received: 15 October 2015 / Revised: 23 March 2016 / Accepted: 9 May 2016
© Springer Science+Business Media New York 2016

Abstract Optimizing eigenvalues of biharmonic equations appears in the frequency control based on density distribution of composite rods and thin plates with clamped or simply supported boundary conditions. In this paper, we use a rearrangement algorithm to find the optimal density distribution which minimizes a specific eigenvalue. We answer the open question regarding optimal density configurations to minimize k -th eigenvalue for clamped rods and analytically show that the optimal configurations are distinct for clamped rods and simply supported rods. Many numerical simulations in both one and two dimensions demonstrate the robustness and efficiency of the proposed approach.

Keywords Rearrangement algorithm · Eigenvalue optimization · Biharmonic equation · Density function · Rods · Thin plates

1 Introduction

Optimization of eigenvalues in problems involving elliptic operators in inhomogeneous media [6, 21] has many applications, including mechanical vibration [1, 4, 5, 11, 12, 15, 17, 18, 20, 21,

Ching-Shan Chou: This author is supported by NSF DMS1253481, Chiu-Yen Kao: This author is partially supported by NSF DMS1318364.

✉ Chiu-Yen Kao
Ckao@cmc.edu

Weitao Chen
weitaoc1@uci.edu

Ching-Shan Chou
chou@math.ohio-state.edu

¹ Department of Mathematics, University of California, Irvine, CA 92697, USA

² Department of Mathematics, The Ohio State University, Columbus, OH 43210, USA

³ Department of Mathematical Sciences, Claremont McKenna College, Claremont, CA 91711, USA

27, 29, 39, 42], optical resonator [26, 28, 31, 33], photonic crystals [13, 16, 19, 25, 34, 35, 40, 43], and population dynamics [22, 24, 32]. Thus far most of the theoretical results and numerical approaches are developed for the applications which can be modeled as extremum problems for eigenvalues of second order elliptic operators. However, most of extremum problems for eigenvalues of fourth order elliptic operators are widely open. Some of major difficulties come from that the solutions of fourth order equations do not necessarily have the maximum principle and sign preserving properties as in second order elliptic equations.

For homogeneous media, many previous works on eigenvalue optimization of fourth order elliptic equations focused on studying the optimal shape which optimizes (minimizes or maximizes) the first eigenvalue [2, 10, 37, 38, 41, 45, 46, 48]. In this paper, we study the minimization of a specific eigenvalue of the simplest fourth order elliptic equation, i.e., biharmonic equation, in inhomogeneous media. This problem comes from the study of frequency control based on density distribution of composite rods and plates in one and two dimensions, respectively. In [1, 17, 18], the authors studied theoretically minimization and maximization of the first eigenvalue for several given materials with fixed volumes and found that the density distribution is a monotone function of the square of the eigenfunction corresponding to the specific eigenvalue to be optimized when the extremum occurs. In [36], numerical approaches based on ideas of rearrangement were proposed to find density configurations of the extremal first eigenvalues.

Here we also use a rearrangement approach [27] to minimize the eigenvalues. Not only the first eigenvalue but also higher eigenvalues are studied. We will answer the open problem 30 mentioned in page 183 of reference [21] regarding the optimal two-phase density distributions for eigenvalue minimization for clamped rods and hinged rods. Since the first eigenfunction of the biharmonic equation with clamped boundary conditions can possibly change sign [8, 9, 44], the optimal density configuration could be much more complicated than the one of the harmonic equation. In this paper, we consider optimization problems in parallel to those studied for harmonic equations. Many numerical results are shown to demonstrate the robustness and efficiency of our numerical approach.

This paper is organized as follows. In Sect. 2, we introduce the biharmonic eigenvalue problems and their known theoretical results. In Sect. 3, we perform an asymptotic analysis to show that the density configurations to minimize a specific eigenvalue of hinged rods and clamped rods are different. In Sect. 4, we present finite difference methods for forward eigenvalue problems and the rearrangement algorithm to minimize a specific eigenvalue. In Sect. 5, numerical simulations on inhomogeneous rods and plates are shown for bang-bang density distribution with both clamped and simply supported boundary conditions. In Sect. 6, we conclude our paper with a discussion.

2 Inhomogeneous Biharmonic Eigenvalue Problems

Let Ω be a bounded open set in \mathbb{R}^N . We consider the minimization problem of the k -th eigenvalue

$$\min_{\rho(x)} \lambda_k$$

of the inhomogeneous clamped plate equation

$$\begin{cases} \Delta^2 u(x) = \lambda \rho(x) u(x) & \text{in } \Omega, \\ u = \frac{\partial u}{\partial n} = 0 & \text{on } \partial \Omega, \end{cases} \quad (1)$$

and the inhomogeneous simply supported plate equation

$$\begin{cases} \Delta^2 u(x) = \lambda \rho(x) u(x) & \text{in } \Omega, \\ u = \Delta u - (1 - \nu) \kappa \frac{\partial u}{\partial n} = 0 & \text{on } \partial \Omega. \end{cases} \tag{2}$$

The operator $\Delta^2 = \Delta \cdot \Delta$ is the biharmonic operator, u is the eigenfunction, λ is the corresponding eigenvalue, and $\rho(x)$ is in the class

$$\mathcal{A}_{\alpha, \beta, \gamma}(\Omega) = \{\rho(x) \in L^\infty(\Omega); \alpha \leq \rho(x) \leq \beta \text{ a.e. in } \Omega, \int_{\Omega} \rho(x) dx = \gamma\},$$

where n denotes the unit outward normal, κ is the curvature, ν is the Poisson’s ratio satisfying $-1 \leq \nu \leq 0.5$, and α, β, γ are given constants. For ease of exposition, the dimension N is chosen to be one or two in this paper. Let (λ_k, u_k) be the k -th eigenpair. Then the variational formulations of the eigenvalues for clamped boundary conditions are

$$\lambda_1(\rho) = \inf_{\psi \in H_0^2(\Omega), \psi \neq 0} \frac{\int_{\Omega} (\Delta \psi)^2 dx}{\int_{\Omega} \rho \psi^2 dx}, \tag{3}$$

and

$$\lambda_k(\rho) = \min_{\substack{E_k \subset H_0^2(\Omega), \\ \text{subspace of dim } k}} \max_{\psi \in E_k, \psi \neq 0} \frac{\int_{\Omega} (\Delta \psi)^2 dx}{\int_{\Omega} \rho \psi^2 dx}, \tag{4}$$

for higher eigenmodes $k \geq 2$. The variational formulations of the eigenvalues for simply supported boundary conditions are

$$\lambda_1(\rho) = \inf_{\psi \in H_0^1(\Omega) \cap H^2(\Omega), \psi \neq 0} \frac{\int_{\Omega} (\Delta \psi)^2 dx - \int_{\partial \Omega} (1 - \nu) \kappa \left(\frac{\partial \psi}{\partial n}\right)^2 dS}{\int_{\Omega} \rho \psi^2 dx}, \tag{5}$$

and

$$\lambda_k(\rho) = \min_{\substack{E_k \subset H_0^1(\Omega) \cap H^2(\Omega), \\ \text{subspace of dim } k}} \max_{\psi \in E_k, \psi \neq 0} \frac{\int_{\Omega} (\Delta \psi)^2 dx - \int_{\partial \Omega} (1 - \nu) \kappa \left(\frac{\partial \psi}{\partial n}\right)^2 dS}{\int_{\Omega} \rho \psi^2 dx}, \tag{6}$$

for higher eigenmodes $k \geq 2$.

When $\rho(x)$ is positive everywhere, (1) and (2) are models used to describe the vibration of a clamped plate and a simply supported plate with the inhomogeneous density function $\rho(x)$, respectively. It is worth pointing out that the simply supported boundary conditions can be simplified to the hinged boundary conditions, where $\Delta u = 0$, in one or two dimensions with homogeneous Dirichlet boundary conditions and zero curvature on the boundary. In the discussion below, we will use the terminology “the hinged boundary conditions” for one-dimensional intervals or two-dimensional rectangular domains. Otherwise, ν will be specified in the simply supported boundary conditions.

In one dimension, the theoretical results [3–5, 42] indicated that the optimal distributions of $\rho(x)$ are of bang-bang type for both boundary conditions. The eigenvalue problem of an inhomogeneous clamped rod is

$$\begin{cases} u^{(4)}(x) = \lambda \rho(x) u(x), & \text{in } [-L, L], \\ u(-L) = u'(-L) = u(L) = u'(L) = 0, \end{cases}$$

and the eigenvalue problem of a hinged (simply supported) rod is

$$\begin{cases} u^{(4)}(x) = \lambda\rho(x)u(x), & \text{in } [-L, L]. \\ u(-L) = u''(-L) = u(L) = u''(L) = 0. \end{cases}$$

Then the unique minimizer $\check{\rho}_1(x)$ (maximizer $\hat{\rho}_1(x)$) of both clamped and hinged extremal eigenvalue problems $\min_{\rho(x)} \lambda(\rho)$ ($\max_{\rho(x)} \lambda(\rho)$) in the class of $\mathcal{A}_{\alpha,\beta,\gamma}$ is

$$\check{\rho}_1(x) = \begin{cases} \alpha, & x \in (-L, -\delta), \\ \beta, & x \in (-\delta, \delta), \\ \alpha, & x \in (\delta, L), \end{cases} \quad \left(\hat{\rho}_1(x) = \begin{cases} \beta, & x \in (-L, -\delta), \\ \alpha, & x \in (-\delta, \delta), \\ \beta, & x \in (\delta, L), \end{cases} \right)$$

where $\delta = (\gamma - 2\alpha L)/(2\beta - 2\alpha)$ ($\delta = (\gamma - 2\beta L)/(2\alpha - 2\beta)$). This optimal distribution is the same as the one for Dirichlet Laplace eigenvalue problem

$$\begin{cases} -u''(x) = \lambda\rho(x)u(x), & \text{in } [-L, L], \\ u(-L) = u(L) = 0, \end{cases}$$

which was discovered by Krein [29]. He also found that optimal distributions for general higher eigenmodes λ_k ($k \geq 2$) of Dirichlet Laplace eigenvalue problem are $2L/k$ -periodic and are defined on each interval

$$\left(-L + \frac{j2L}{k}, -L + \frac{(j+1)2L}{k} \right), \quad j = 0, \dots, k-1,$$

by

$$\rho_k(x) = \check{\rho}_1(kx - (2j+1-k)L) \quad (\rho_k(x) = \hat{\rho}_1(kx - (2j+1-k)L)). \quad (7)$$

Banks [4] found that the optimal distributions for λ_k for the hinged rod problem are exactly the same as (7). However, the optimal density distribution for the clamped rod problem remains an open question [21, p.183].

In two or higher dimensions, the problem (1) was considered recently in [1, 17, 18]. The authors studied minimization and maximization of the first eigenvalue for several given materials of fixed volumes. The existence of minimizers in the family of all measurable functions which are rearrangements of a given function were proved for both clamped and hinged boundary conditions; however, the existence of maximizers can be proved only for domains Ω such that the operator is positive preserving, i.e., $u \geq 0$ if $\Delta^2 u = f$ in Ω with clamped boundary conditions for any given $f \geq 0$. Furthermore, the extremum occurs when the density function is a monotone increasing (decreasing) function of the square of the eigenfunction corresponding to the eigenvalue which is to be minimized (maximized). This implies that the material with higher (lower) density must overlap with where the magnitude of eigenfunction is larger (smaller).

3 Open Question: Is the Minimizer of Hinged Rod Also the Minimizer of Clamped Rod?

In this section, we only consider the minimization problem. A similar approach can be applied to the maximization problem. The minimizers for all eigenmodes with hinged boundary conditions in one dimension are described in (7). The density in the optimal configuration is periodically distributed with higher density in the center within each period. However, the analytic form of the minimizer associated with clamped boundary conditions is unknown

[21]. Based on numerical simulations shown in Sect. 5.1, we notice that unlike the hinged boundary conditions, the minimizer of k -th eigenvalue, $k \geq 2$, with clamped boundary conditions, does not have periodicity; in other words, the minimizer of the hinged rod cannot be the minimizer of the clamped rod. However, it is not trivial to compute the explicit formula of the minimizers for the clamped rod. Here we attempt to prove that the minimizer of the hinged rod is not the minimizer of the clamped rod, and it suffices to show that the minimizer of hinged rod cannot give the minimal eigenvalue in a subspace of the density distributions satisfying the constraint.

Without loss of generality, we consider the problem on the interval $[-1, 1]$ with the constraint that half of the rod is of high density, and we search for a minimizer of λ_2 in the subspace of density functions satisfying

$$\left\{ \rho(x) \in \mathcal{A}_{\alpha,\beta,\gamma}(\Omega) : \rho(x) = \begin{cases} \beta, & \text{if } x \in [-c - \frac{1}{4}, -c + \frac{1}{4}] \cup [c - \frac{1}{4}, c + \frac{1}{4}], \\ \alpha, & \text{otherwise,} \end{cases} \right\} \quad (8)$$

where $c \in (\frac{1}{4}, \frac{3}{4})$ and $\gamma = \alpha + \beta$. Note that $\rho(x)$ is the minimizer of the hinged rod if $c = \frac{1}{2}$. Our goal is to show that the eigenvalue λ_2 obtained at $c = \frac{1}{2}$ is not the minimum in the interval $(\frac{1}{4}, \frac{3}{4})$ when clamped boundary conditions are imposed. In the following, we will prove this by using an asymptotic analysis based on the assumption that the densities of two materials are sufficiently close.

Let $\alpha = \rho$, $\beta = \rho + \epsilon$, where ρ is a positive constant and ϵ is a small positive number. Assume (μ, v) is the second eigenpair of the eigenvalue problem with a homogeneous density ρ . Denote the perturbed density by

$$\rho_\epsilon(x) = \begin{cases} \rho + \epsilon, & \text{if } x \in [-c - \frac{1}{4}, -c + \frac{1}{4}] \cup [c - \frac{1}{4}, c + \frac{1}{4}], \\ \rho, & \text{otherwise.} \end{cases}$$

Then the perturbed clamped plate problem is

$$\begin{cases} (u_\epsilon)^{(4)}(x) = \lambda_\epsilon \rho_\epsilon u_\epsilon(x), & \text{in } [-1, 1], \\ u_\epsilon(-1) = u_\epsilon(1) = u'_\epsilon(-1) = u'_\epsilon(1) = 0, \end{cases}$$

and its second eigenpair $(\lambda_\epsilon, u_\epsilon)$ can be formally expanded as ([7, 23])

$$\begin{aligned} \lambda_\epsilon &= \mu + \epsilon \mu_1 + \epsilon^2 \mu_2 + \mathcal{O}(\epsilon^3), \\ u_\epsilon &= v + \epsilon v_1 + \epsilon^2 v_2 + \mathcal{O}(\epsilon^3). \end{aligned}$$

The weak formulation is

$$\left((u_\epsilon)^{(3)} \psi - (u_\epsilon)'' \psi' \right) \Big|_{-1}^1 + \int_{-1}^1 (u_\epsilon)'' \psi'' dx = \lambda_\epsilon \int_{-1}^1 \rho_\epsilon u_\epsilon \psi dx, \quad (9)$$

where ψ is a smooth test function. The right-hand side equals

$$\lambda_\epsilon \int_{-1}^1 \rho_\epsilon u_\epsilon \psi dx = \lambda_\epsilon \int_{-1}^1 \rho u_\epsilon \psi dx + \lambda_\epsilon \int_{-1}^1 (\rho_\epsilon - \rho) u_\epsilon \psi dx.$$

Moreover,

$$\int_{-1}^1 (\rho_\epsilon - \rho) u_\epsilon \psi dx = \int_{-c-\frac{1}{4}}^{-c+\frac{1}{4}} \epsilon v \psi dx + \int_{c-\frac{1}{4}}^{c+\frac{1}{4}} \epsilon v \psi dx + \mathcal{O}(\epsilon^2).$$

By comparing ϵ^0 order term in Eq. (9), we have

$$\mathcal{O}(\epsilon^0) : \left(v^{(3)}\psi - v''\psi' \right) \Big|_{-1}^1 + \int_{-1}^1 v''\psi'' dx = \mu \int_{-1}^1 \rho v\psi dx. \tag{10}$$

This equality naturally holds for the eigenpair (μ, v) of the homogeneous eigenvalue problem

$$\begin{cases} v^{(4)}(x) = \mu\rho v, & \text{in } [-1, 1], \\ v(-1) = v(1) = \frac{\partial v}{\partial n}(-1) = \frac{\partial v}{\partial n}(1) = 0 \end{cases}$$

Compare the ϵ^1 order term:

$$\begin{aligned} \mathcal{O}(\epsilon^1) : & \left((v_1)^{(3)}\psi - (v_1)''\psi' \right) \Big|_{-1}^1 + \int_{-1}^1 (v_1)''\psi'' dx \\ & = \mu \int \rho v_1\psi dx + \mu_1 \int_{-1}^1 \rho v\psi dx + \mu \left(\int_{-c-\frac{1}{4}}^{-c+\frac{1}{4}} v\psi dx + \int_{c-\frac{1}{4}}^{c+\frac{1}{4}} v\psi dx \right). \end{aligned} \tag{11}$$

Plugging $\psi = v_1$ into Eq. (10), it yields

$$\int_{-1}^1 v''v_1'' dx = \mu \int_{-1}^1 \rho v v_1 dx. \tag{12}$$

Plugging $\psi = v$ into Eq. (11) and using the equality (12) lead to

$$\mu_1 \int_{-1}^1 \rho v^2 dx + \mu \left(\int_{-c-\frac{1}{4}}^{-c+\frac{1}{4}} v^2 dx + \int_{c-\frac{1}{4}}^{c+\frac{1}{4}} v^2 dx \right) = 0.$$

Hence,

$$\mu_1 = \frac{-\mu \left(\int_{-c-\frac{1}{4}}^{-c+\frac{1}{4}} v^2 dx + \int_{c-\frac{1}{4}}^{c+\frac{1}{4}} v^2 dx \right)}{\int_{-1}^1 \rho v^2 dx}.$$

It is well known that the eigenfunctions for the homogeneous clamped rod are given by

$$\phi_n(x) = \begin{cases} \cosh\left(r_{1, \frac{n+1}{2}}\right) \cos\left(r_{1, \frac{n+1}{2}}x\right) - \cos\left(r_{1, \frac{n+1}{2}}\right) \cosh\left(r_{1, \frac{n+1}{2}}x\right) & \text{when } n \text{ is odd,} \\ \sinh\left(r_{2, \frac{n}{2}}\right) \sin\left(r_{2, \frac{n}{2}}x\right) - \sin\left(r_{2, \frac{n}{2}}\right) \sinh\left(r_{2, \frac{n}{2}}x\right) & \text{when } n \text{ is even,} \end{cases}$$

where $r_{1,m}$ and $r_{2,m}$ are the m -th positive roots of $\tan(r) + \tanh(r) = 0$ and $\tan(r) - \tanh(r) = 0$, respectively, and the corresponding eigenvalues are $\lambda_{2m-1} = r_{1,m}^4/\rho$ and $\lambda_{2m} = r_{2,m}^4/\rho$.

Note that on each period $\left[\frac{k\pi}{2}, \frac{(k+2)\pi}{2} \right]$, $\tan(x)$ intercepts with $\tanh(x)$ and $-\tanh(x)$ once, respectively, giving those corresponding eigenvalues.

Here we consider the second eigenfunction of $v^{(4)} = \mu\rho v$, which is

$$v = \sinh(r_{2,1}) \sin(r_{2,1}x) - \sin(r_{2,1}) \sinh(r_{2,1}x),$$

where $\pi < r_{2,1} < \frac{3\pi}{2}$ and $r_{2,1} \approx 3.9266$. Since we know that $\tan\left(\frac{7\pi}{6}\right) = \frac{1}{\sqrt{3}}$, $\tan\left(\frac{5\pi}{4}\right) = 1$ and $\tanh\left(\frac{7\pi}{6}\right) > \frac{1}{2}$, the root must satisfy $\frac{7\pi}{6} < r_{2,1} < \frac{5\pi}{4}$.

Due to the fact that $\mu > 0$ and v is an odd function,

$$\mu_1 = \frac{-2\mu \int_{c-\frac{1}{4}}^{c+\frac{1}{4}} v^2 dx}{\int_{-1}^1 \rho v^2 dx},$$

and

$$\frac{\partial \lambda_\epsilon}{\partial c} = \epsilon \frac{\partial \mu_1}{\partial c} + \mathcal{O}(\epsilon^2) = \frac{-2\epsilon\mu}{\int_{-1}^1 \rho v^2 dx} \frac{\partial}{\partial c} \left(\int_{c-\frac{1}{4}}^{c+\frac{1}{4}} v^2 dx \right) + \mathcal{O}(\epsilon^2).$$

Therefore, minimizing the leading order term of λ_ϵ is equivalent to maximizing $\int_{c-\frac{1}{4}}^{c+\frac{1}{4}} v^2 dx$ when ϵ is small. Since

$$\int_{c-\frac{1}{4}}^{c+\frac{1}{4}} v^2 dx = \int_{c-\frac{1}{4}}^{c+\frac{1}{4}} (\sinh(r_{2,1}) \sin(r_{2,1}x) - \sin(r_{2,1}) \sinh(r_{2,1}x))^2 dx,$$

then

$$\begin{aligned} \frac{\partial}{\partial c} \int_{c-\frac{1}{4}}^{c+\frac{1}{4}} v^2 dx \Big|_{c=\frac{1}{2}} &= \left(\sinh(r_{2,1}) \sin\left(\frac{3}{4}r_{2,1}\right) - \sin(r_{2,1}) \sinh\left(\frac{3}{4}r_{2,1}\right) \right. \\ &\quad \left. + \sinh(r_{2,1}) \sin\left(\frac{1}{4}r_{2,1}\right) - \sin(r_{2,1}) \sinh\left(\frac{1}{4}r_{2,1}\right) \right) \\ &\quad \cdot \left(\sinh(r_{2,1}) \sin\left(\frac{3}{4}r_{2,1}\right) - \sin(r_{2,1}) \sinh\left(\frac{3}{4}r_{2,1}\right) \right) \\ &\quad - \sinh(r_{2,1}) \sin\left(\frac{1}{4}r_{2,1}\right) + \sin(r_{2,1}) \sinh\left(\frac{1}{4}r_{2,1}\right). \end{aligned}$$

Note that

$$\begin{aligned} &\sinh(r_{2,1}) \sin\left(\frac{3}{4}r_{2,1}\right) - \sin(r_{2,1}) \sinh\left(\frac{3}{4}r_{2,1}\right) \\ &\quad + \sinh(r_{2,1}) \sin\left(\frac{1}{4}r_{2,1}\right) - \sin(r_{2,1}) \sinh\left(\frac{1}{4}r_{2,1}\right) \\ &= \sinh(r_{2,1}) \left(\sin\left(\frac{3}{4}r_{2,1}\right) + \sin\left(\frac{1}{4}r_{2,1}\right) \right) \\ &\quad - \sin(r_{2,1}) \left(\sinh\left(\frac{3}{4}r_{2,1}\right) + \sinh\left(\frac{1}{4}r_{2,1}\right) \right) > 0, \end{aligned}$$

because $\sinh(r_{2,1}) > 0$, $\sin\left(\frac{3}{4}r_{2,1}\right) + \sin\left(\frac{1}{4}r_{2,1}\right) > 0$, $\sin(r_{2,1}) < 0$ and $\sinh\left(\frac{3}{4}r_{2,1}\right) + \sinh\left(\frac{1}{4}r_{2,1}\right) > 0$ for $\frac{7\pi}{6} < r_{2,1} < \frac{5\pi}{4}$. We also have

$$\begin{aligned} &\sinh(r_{2,1}) \sin\left(\frac{3}{4}r_{2,1}\right) - \sin(r_{2,1}) \sinh\left(\frac{3}{4}r_{2,1}\right) \\ &\quad - \sinh(r_{2,1}) \sin\left(\frac{1}{4}r_{2,1}\right) + \sin(r_{2,1}) \sinh\left(\frac{1}{4}r_{2,1}\right) \\ &= 8 \cos\left(\frac{r_{2,1}}{2}\right) \cosh\left(\frac{r_{2,1}}{2}\right) \sinh\left(\frac{r_{2,1}}{4}\right) \sin\left(\frac{r_{2,1}}{4}\right) \left[\cosh\left(\frac{r_{2,1}}{4}\right) - \cos\left(\frac{r_{2,1}}{4}\right) \right] < 0, \end{aligned}$$

because $\cos\left(\frac{r_{2,1}}{2}\right) < 0$, $\cosh\left(\frac{r_{2,1}}{2}\right) > 0$, $\sinh\left(\frac{r_{2,1}}{4}\right) > 0$, $\sin\left(\frac{r_{2,1}}{4}\right) > 0$ and $\cosh\left(\frac{r_{2,1}}{4}\right) - \cos\left(\frac{r_{2,1}}{4}\right) > 0$ for $\frac{7\pi}{6} < r_{2,1} < \frac{5\pi}{4}$.

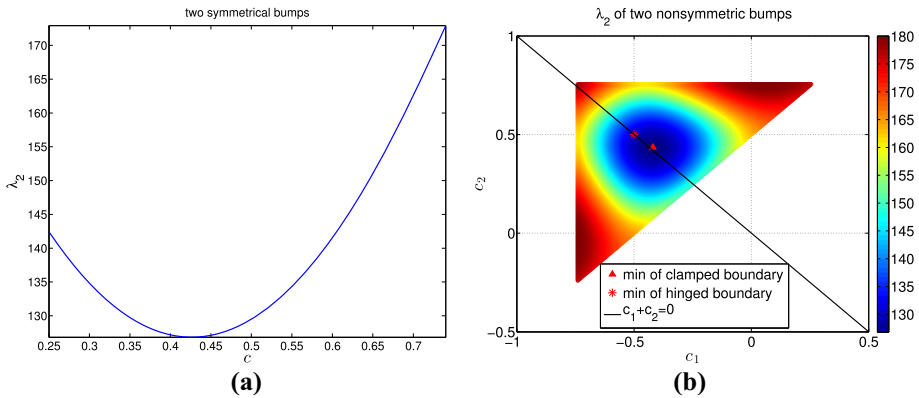


Fig. 1 Search for the minimizer of λ_2 for clamped boundary conditions by perturbing centers of two equal bumps. **a** Plot of second clamped eigenvalue with respect to c , center of symmetric high density regions; **b** plot of second clamped eigenvalue with respect to c_i 's, centers of non-symmetric high density regions

Therefore,

$$\left. \frac{\partial}{\partial c} \int_{c-\frac{1}{4}}^{c+\frac{1}{4}} v^2 dx \right|_{c=\frac{1}{2}} < 0 \text{ and } \left. \frac{\partial \lambda_\epsilon}{\partial c} \right|_{c=\frac{1}{2}} > 0.$$

This completes the proof that λ_ϵ is not minimized at $c = \frac{1}{2}$. Now we can conclude that: (1) when ϵ is small, the minimizer of the hinged rod is not the minimizer of the clamped rod; (2) decreasing c near $\frac{1}{2}$ can give a smaller second eigenvalue in the subspace of density functions satisfying Eq. (8). Actually, these conclusions are consistent with what we observe numerically. We perform a search for the minimizer in the same subspace by calculating the second eigenmode of the clamped eigenvalue problem for different values of c between $\frac{1}{4}$ and $\frac{3}{4}$ with $\alpha = 1$ and $\beta = 2$. The plot of the second eigenvalue with respect to c is shown in Fig. 1a. We can see that the second eigenvalue is increasing with respect to c at $\frac{1}{2}$ and the minimum is achieved between 0.4 and 0.45. We also perform a similar search in a larger subspace of density functions such that the compartments of high density with equal lengths are not necessarily symmetric about 0. The centers of the high density compartments, denoted by c_1 and c_2 , must satisfy $-\frac{1}{2} \leq c_1 + \frac{1}{4} \leq c_2 - \frac{1}{4} \leq \frac{1}{2}$. The search is thus implemented in two dimensions in terms of c_1 and c_2 by computing the second eigenvalue corresponding to the density function

$$\rho(x) = \begin{cases} 2 & \text{if } x \in [c_1 - \frac{1}{4}, c_1 + \frac{1}{4}] \cup [c_2 - \frac{1}{4}, c_2 + \frac{1}{4}], \\ 1 & \text{otherwise.} \end{cases}$$

The result is shown in Fig. 1b. The star marks the minimizer of the hinged rod and the triangle is for the clamped rod. They are obviously distinct. Numerically we can also see that the minimizer of the clamped rod is on the line $c_1 + c_2 = 0$, i.e., the high density regions are symmetric with respect to zero.

Remark 1 In fact, if $\mu_1 = 0$, c satisfies either

$$\sinh(r_{2,1}) \sin\left(\frac{1}{4}r_{2,1}\right) \cos(r_{2,1}c) - \sin(r_{2,1}) \sinh\left(\frac{1}{4}r_{2,1}\right) \cosh(r_{2,1}c) = 0$$

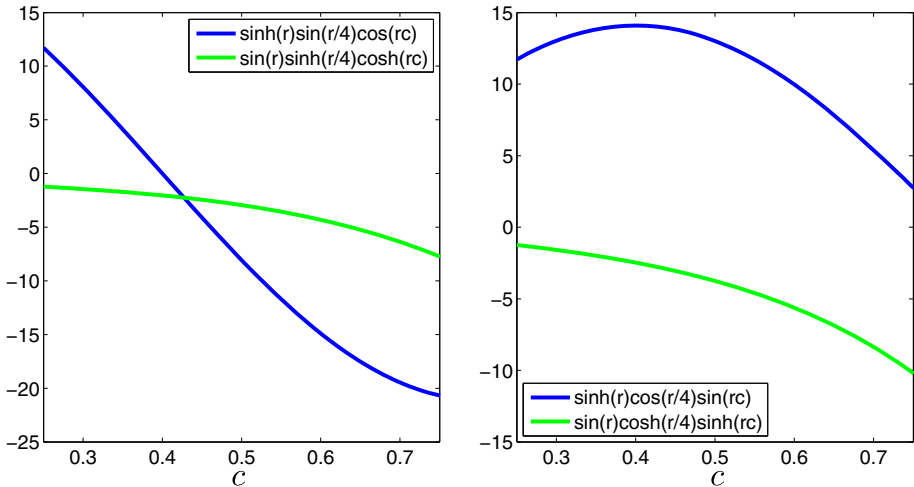


Fig. 2 The plots of $\sinh(r_{2,1}) \sin\left(r_{2,1}\frac{1}{4}\right) \cos(r_{2,1}c)$ and $\sin(r_{2,1}) \sinh\left(\frac{1}{4}r_{2,1}\right) \cosh(r_{2,1}c)$ (left), $\sinh(r_{2,1}) \cos\left(\frac{1}{4}r_{2,1}\right) \sin(r_{2,1}c)$ and $\sin(r_{2,1}) \cosh\left(\frac{1}{4}r_{2,1}\right) \sinh(r_{2,1}c)$ (right) in $\left[\frac{1}{4}, \frac{3}{4}\right]$

or

$$\sinh(r_{2,1}) \cos\left(\frac{1}{4}r_{2,1}\right) \sin(r_{2,1}c) - \sin(r_{2,1}) \cosh\left(\frac{1}{4}r_{2,1}\right) \sinh(r_{2,1}c) = 0.$$

The first equation has only one root which is approximately 0.4272 while the second equation has no roots in $\left[\frac{1}{4}, \frac{3}{4}\right]$, as shown in Fig. 2.

Remark 2 This approach can be applied straightforwardly to the proof of a distinct minimizer of higher eigenmode $\lambda_k, k \geq 3$, for a clamped rod from that of a hinged rod. For example, for the third eigenvalue, if searching the minimizer in the subspace such that the high density region consists of three sub-intervals with equal lengths, with one of them centered at zero and the other two symmetric about zero, we can assume

$$\rho_\epsilon(x) = \begin{cases} \rho + \epsilon, & x \in [-c - \frac{1}{6}, -c + \frac{1}{6}] \cup [-\frac{1}{6}, \frac{1}{6}] \cup [c - \frac{1}{6}, c + \frac{1}{6}], \\ \rho, & \text{otherwise.} \end{cases}$$

The derivation is similar except that the third eigenfunction of the homogeneous clamped rod satisfies

$$v = \cosh(r_{1,2}) \cos(r_{1,2}x) - \cos(r_{1,2}) \cosh(r_{1,2}x),$$

where $r_{1,2} = 5.4978$ is the second root of $\tan(x) + \tanh(x) = 0$. Minimizing the leading order term of λ_ϵ is equivalent to maximizing $\int_{c-\frac{1}{6}}^{c+\frac{1}{6}} v^2 dx$ because v is even and ϵ is small. Setting the first order derivative equal to zero gives

$$\begin{aligned} \frac{\partial}{\partial c} \int_{c-\frac{1}{6}}^{c+\frac{1}{6}} v^2 dx &= \left(\cosh(r_{1,2}) \cos\left(r_{1,2}\left(c + \frac{1}{6}\right)\right) - \cos(r_{1,2}) \cosh\left(r_{1,2}\left(c + \frac{1}{6}\right)\right) \right)^2 \\ &\quad - \left(\cosh(r_{1,2}) \cos\left(r_{1,2}\left(c - \frac{1}{6}\right)\right) - \cos(r_{1,2}) \cosh\left(r_{1,2}\left(c - \frac{1}{6}\right)\right) \right)^2 = 0, \end{aligned}$$

i.e., either

$$\cosh(r_{1,2}) \cos(r_{1,2}c) \cos\left(\frac{1}{6}r_{1,2}\right) - \cos(r_{1,2}) \cosh(r_{1,2}c) \cosh\left(\frac{1}{6}r_{1,2}\right) = 0$$

or

$$\cosh(r_{1,2}) \sin(r_{1,2}c) \sin\left(\frac{1}{6}r_{1,2}\right) + \cos(r_{1,2}) \sinh(r_{1,2}c) \sinh\left(\frac{1}{6}r_{1,2}\right) = 0.$$

With $r_{1,2} = 5.4978$, the first equation has no roots and the second equation has only one root, which is $c \approx 0.5892$. This indicates that the first order approximation of the minimizer of a clamped rod in this subspace is achieved roughly when the centers of the three intervals are approximately located at $-0.5892, 0$ and 0.5892 . In contrast, the centers in the minimizer of a hinged rod are located at $-\frac{2}{3}, 0, \frac{2}{3}$, respectively. Thus the minimizer of a hinged rod is not the minimizer of a clamped rod for the minimization of the third eigenvalue.

4 Numerical Discretization and Optimization

The numerical approach for extremal eigenvalue problems consists of two parts: (1) the forward solver on a given domain: given the density function ρ , find its corresponding eigenvalues λ_k and eigenfunctions u_k ; (2) the optimization solver: given eigenvalues and eigenfunctions under the current density function, determine a new distribution of the density function ρ such that the objective function, i.e., λ_k , decreases. For simplicity, we perform the finite difference calculations on one-dimensional intervals and two-dimensional rectangular, circular, and annular domains. Problems on general domains can be solved similarly via finite element approaches [27,36].

4.1 Finite Difference Methods for Forward Problems

The finite difference discretization on different domains adopts distinct treatments to avoid singularities and impose boundary conditions precisely. On a one-dimensional interval or a two-dimensional rectangular domain, we follow the regular finite difference method to discretize the equation. On a sphere or an annulus, the discretization is performed after transforming the equation into polar coordinates. The details of finite difference discretization for biharmonic eigenvalue problems equipped with clamped or simply supported boundary conditions on domains of different shapes are provided in “Appendices 1, 2, 3”.

Overall, the discretization of biharmonic eigenvalue problems on square, circular, and annular domains, all lead to a square matrix, denoted by A , and the discretization of the right-hand-side term $\rho(x)$ will form a diagonal matrix, denoted by B , with the corresponding density $\rho_{i,j}$ which orders in the same way as $U_{i,j}$ along the diagonal. The resulting generalized eigenvalue problem $AU = \Lambda BU$, with Λ being the diagonal eigenvalue matrix, is then solved by Arnoldi’s method [30] to obtain the first few eigenvalues and eigenfunctions.

4.2 Rearrangement Algorithm for Minimization of Eigenvalues

In order to optimize the k -th eigenvalue, we use the fully sorting algorithm which was proposed to solve optimization problems in harmonic eigenvalue equations [27]. Define the Rayleigh quotient of the biharmonic operator as

$$R[\psi] := \frac{\int_{\Omega} (\Delta\psi)^2 dx}{\int_{\Omega} \rho(x)\psi^2(x)dx}$$

if clamped boundary conditions are imposed, or

$$R[\psi] := \frac{\int_{\Omega} (\Delta\psi)^2 dx - \int_{\partial\Omega} (1-\nu)\kappa(\frac{\partial\psi}{\partial n})^2 dS}{\int_{\Omega} \rho(x)\psi^2(x)dx}$$

if simply supported boundary conditions are imposed. Note that in both formulas the density ρ appears only in the denominator of $R[\psi]$, so we denote the numerator of $R[\psi]$ by $D(\psi)$. Let $B(\Omega) = H_0^1(\Omega) \cap H^2(\Omega)$ stand for simply supported boundary conditions and $B(\Omega) = H_0^2(\Omega)$ for clamped boundary conditions. The constraint is given by $\int_{\Omega} \rho(x)dx = \gamma$, where γ is some constant. Under this constraint, once the densities of two materials are given, the area percentages for each of them are determined. The fully sorting algorithm described below can guarantee the density constraint is always satisfied. Consider the minimization problem for the first eigenvalue

$$\min_{\rho(x)} \lambda_1 = \min_{\rho(x)} \min_{\psi \in B(\Omega)} \frac{D(\psi)}{\int_{\Omega} \rho(x)\psi^2(x)dx}$$

and

$$\min_{\rho(x)} \lambda_k = \min_{\rho(x)} \min_{E_k \subset B(\Omega), \text{subspace of dim } k} \max_{\psi \in E_k, \psi \neq 0} \frac{D(\psi)}{\int_{\Omega} \rho(x)\psi^2(x)dx}$$

for $k > 1$. Assume that the eigenfunctions are normalized by $\int_{\Omega} \rho(x)\psi^2(x)dx = 1$. At the i -th iteration, the density function is denoted by ρ^i . Use the forward problem solver described in the previous section to find the corresponding eigenvalue $\lambda_k(\rho^i)$ and the eigenfunction $u_k(\rho^i)$. For simplicity, denote them by the eigenpair $(\lambda_{k,i}, u_{k,i})$. Thus

$$\lambda_{k,i} = \frac{D(u_{k,i})}{\int_{\Omega} \rho^i u_{k,i}^2 dx}$$

Our goal becomes to find a density function $\rho(x)$ such that it can maximize the integral in the denominator, namely,

$$\int_{\Omega} \rho(x)u_{k,i}^2 dx. \tag{13}$$

Suppose ρ^{i+1} is a new guess, such that

$$\int_{\Omega} \rho^{i+1} u_{k,i}^2 dx \geq \int_{\Omega} \rho^i u_{k,i}^2 dx,$$

then a new estimate for $\lambda_{k,i+1}$ will be smaller because

$$\begin{aligned} \lambda_{1,i+1} &= \min_{\psi \in B(\Omega), \psi \neq 0} \frac{D(\psi)}{\int_{\Omega} \rho^{i+1} \psi^2(x)dx} = \frac{D(u_{1,i+1})}{\int_{\Omega} \rho^{i+1} u_{1,i+1}^2(x)dx} \\ &\leq \frac{D(u_{1,i})}{\int_{\Omega} \rho^{i+1} u_{1,i}^2(x)dx} \leq \frac{D(u_{1,i})}{\int_{\Omega} \rho^i u_{1,i}^2(x)dx} = \lambda_{1,i} \end{aligned} \tag{14}$$

and

$$\begin{aligned} \lambda_{k,i+1} &= \min_{\substack{E_k \subset B(\Omega), \\ \text{subspace of dim } k}} \max_{\psi \in E_k, \psi \neq 0} \frac{D(\psi)}{\int_{\Omega} \rho^{i+1} \psi^2(x) dx} \\ &= \frac{D(u_{k,i+1})}{\int_{\Omega} \rho^{i+1} u_{k,i+1}^2(x) dx} \leq \frac{D(u_{k,i})}{\int_{\Omega} \rho^{i+1} u_{k,i}^2(x) dx} \leq \frac{D(u_{k,i})}{\int_{\Omega} \rho^i u_{k,i}^2(x) dx} = \lambda_{k,i} \end{aligned} \quad (15)$$

for $k > 1$ whenever $u_{k,i}$ does not belong to the subspace spanned by $\{u_{1,i+1}, \dots, u_{k-1,i+1}\}$. In fact, $u_{k,i}$ never lies in the subspace of lower eigenmodes associated with ρ^{i+1} in our numerical tests. Therefore, the monotone decreasing sequence $\{\lambda_{k,i}\}$ determined by Eq. (14) and (15) must converge since it is bounded below. The success of this procedure depends on whether we can find a density function so that it maximizes the integral (13). By using the finite difference approximation, the discretized eigenfunction U_k and the density function are written into column vectors

$$\begin{aligned} U_k &= (U_{k1}, U_{k2}, \dots, U_{kN})^T, \\ \rho &= (\rho_1, \rho_2, \dots, \rho_N)^T, \end{aligned}$$

where N is the total number of nodal points. Consequently, the problem becomes to maximize the discretization of (13)

$$\sum_{j=1, \dots, N} \rho_j U_{kj}^2 \Delta x^2 \quad (16)$$

subject to the constraint $\sum_{j=1, \dots, N} \rho_j \Delta x^2 = \gamma$ if Ω is a square. This optimization can be solved by using the following rearrangement inequality.

Rearrangement Inequality [47]: Let

$$a_1 \leq a_2 \leq \dots \leq a_n \text{ and } b_1 \leq b_2 \leq \dots \leq b_n$$

be ordered sequences of real numbers. The inequality

$$a_n b_1 + \dots + a_1 b_n \leq a_{\sigma(1)} b_1 + \dots + a_{\sigma(n)} b_n \leq a_1 b_1 + \dots + a_n b_n$$

holds for every choice of permutation σ on $1, 2, \dots, n$.

This rearrangement inequality indicates that we could optimize the sum in (16) if we arrange ρ_i in the same order as that of U_{kj}^2 . Practically, this means to place higher density material in the region where U_{kj}^2 is larger to maximize the sum, or to place lower density material in the region where U_{kj}^2 is larger to minimize the sum.

Remark 3 The rearrangement method we describe above is essentially an alternating optimization algorithm with respect to ρ (rearrangement) and u (Rayleigh principle). The efficiency of the algorithm is mainly due to the exact solution of the problem with respect to a fixed u .

Remark 4 This fully sorting algorithm can be directly applied to solve simple λ_k for $k \geq 1$. However, it is possible that the k -th eigenvalue becomes multiple, that is, it collides with its neighboring eigenvalues. When this happens, multiple eigenfunctions need to be considered while updating the density function: instead of the order of U_{kj}^2 , we should arrange ρ_j in the order of the convex combination $\sum_{s=0}^c \alpha_s U_{(k-s)j}^2$ where the real numbers α_s 's satisfy $\alpha_s \geq 0$

and $\sum_{s=0}^c \alpha_s = 1$ if $\lambda_{k-c}, \dots, \lambda_k$ collide. One can perform an optimization algorithm to find the optimal α_s 's which give the largest integral (13) or simply choose a combination such that the integral increases at each iteration.

Remark 5 If Ω is a circular or annular domain, the numerical evaluation of the constraint is different because each cell is a small sector instead of a square (a Jacobian needs to be multiplied).

We summarize the minimization algorithm in Algorithm 1.

Algorithm 1 Fully sorting algorithm for minimization of λ_k

Require: Initial guess for $\rho(x)$

Solve the elliptic eigenvalue problem by the forward finite difference method

while $\rho(x)$ is not optimal **do**

if the eigenvalue λ_k is colliding with its neighbors $\lambda_{k-c}, \dots, \lambda_{k-1}$ **then**

 sort the linear combination $\sum_{s=0}^c \alpha_s U_{(k-s)j}^2$ with $\sum_{s=0}^c \alpha_s = 1$ in descending order.

else

 sort U_{kj}^2 in descending order

end if

 Assign the high density to the points corresponding to larger values of the sorted vector and low density to smaller values such that the area of the high density region satisfies the constraint.

if $\|\rho - \rho_{\text{new}}\| = 0$ **then**

 Stop

else

 solve the elliptic eigenvalue problem with ρ_{new}

$\rho = \rho_{\text{new}}$

end if

end while

The computational complexity per iteration in the algorithm is mostly determined by Arnoldi iteration which is used to solve forward eigenvalue problems. Generally, the computational complexity of Arnoldi iteration is $O(k^2N + kN^2)$, where k is the number of eigenvalues calculated and N is the matrix size, when solving $Ax = \lambda Bx$. The $O(kN^2)$ cost is due to the computation of $B^{-1}Ax$ at each Arnoldi iteration while the $O(k^2N)$ is due to the orthogonalization of the Krylov subspace vector. Since A is a block-tridiagonal matrix and B is a diagonal matrix, the computation of $B^{-1}Ax$ is reduced to $O(kN)$. The computational complexity per iteration is reduced to $O(k^2N + kN)$. As to how fast the rearrangement algorithm converges, the numerical results shown in [27] indicate that rearrangement algorithm requires much less iterations (usually less than 10 iterations) than the gradient descent approaches based on shape derivative information (a couple hundred iterations).

5 Simulation Results

In this section, we will show results of the fully sorting algorithm to minimize λ_k for k ranging from 1 to 5 on a square, elongated rectangle, circle, and an annulus. It is worth pointing out that even for the principle eigenmode on a rectangular domain, the eigenfunction may oscillate near a corner and experience sign changing analytically [8,9,44]. However, since the oscillation occurs near a corner within the distance of 10^{-3} with the amplitude below 10^{-10} , only very high precision method on a fine mesh can capture it numerically. This kind of behavior also needs further study on more general domains and for higher eigenmodes,

which is beyond the scope of this paper. In the following numerical simulations, we will consider rods and plates consisting of two different densities and the percentage of lower density region exceeds a certain threshold so that the optimal density configuration is more regular. We expect that the optimal density will become much more complicated when the sign changing effect cannot be ignored.

5.1 Minimization of λ_k on an Interval

Consider the eigenvalue problems (1) and (2) on $[-1, 1]$. First, we test the order of accuracy of the forward solver to compute the eigenvalues $\lambda_k, k = 1, \dots, 6$, of the discretized operator described in Appendix with $\alpha = 1, \beta = 2, \gamma = 3$, and the support of the low density material in the middle. The tested mesh sizes are $h = \frac{1}{100}, \frac{1}{200}, \frac{1}{400}$. The results are shown in Tables 1 and 2. The second order accuracy is clearly observed as the second order central difference scheme is used to approximate the derivatives with hinged and clamped boundary conditions.

We apply the fully sorting algorithm to minimize $\lambda_k, k = 1, 2, 3, 4, 5, 6$ with clamped and hinged boundary conditions with the initial density function mentioned above in the accuracy test. The analytic expression of the optimal density function for the minimizer of a hinged rod has been derived in [21] and it has the periodic configuration in one dimension, shown in Fig. 3. However, the results for clamped boundary conditions shown in Fig. 4 indicate that only the minimizer of the first eigenvalue is the same as that of a hinged rod; for the second eigenmode, there are also two symmetric high density regions in the minimizer's profile, which distinguishes from that of a hinged rod by the non-periodicity; for higher eigenmodes, the sizes of high density regions are not uniform and the bumps farthest from the center

Table 1 Accuracy test for the first six eigenvalues on $[-1, 1]$ with hinged boundary conditions

	$h = \frac{1}{100}$	$h = \frac{1}{200}$	$h = \frac{1}{400}$	$\log_2 \left \frac{u_h - u_{\frac{h}{2}}}{u_{\frac{h}{2}} - u_{\frac{h}{4}}} \right $
λ_1	5.146887	5.147142	5.147205	2.00
λ_2	64.584145	64.590827	64.592497	2.00
λ_3	322.810183	322.888050	322.907520	2.00
λ_4	1124.788345	1125.391246	1125.542012	2.00
λ_5	2724.768224	2727.085277	2727.664785	2.00
λ_6	5323.050869	5328.536361	5329.908507	2.00

Table 2 Accuracy test for the first six eigenvalues on $[-1, 1]$ with clamped boundary conditions

	$h = \frac{1}{100}$	$h = \frac{1}{200}$	$h = \frac{1}{400}$	$\log_2 \left \frac{u_h - u_{\frac{h}{2}}}{u_{\frac{h}{2}} - u_{\frac{h}{4}}} \right $
λ_1	28.627477	28.632999	28.634379	2.00
λ_2	175.589137	175.656833	175.673764	2.00
λ_3	598.313218	598.644725	598.727649	2.00
λ_4	1731.976372	1733.570086	1733.968832	2.00
λ_5	4023.562912	4029.347445	4030.795288	2.00
λ_6	7482.235317	7495.542230	7498.874337	2.00

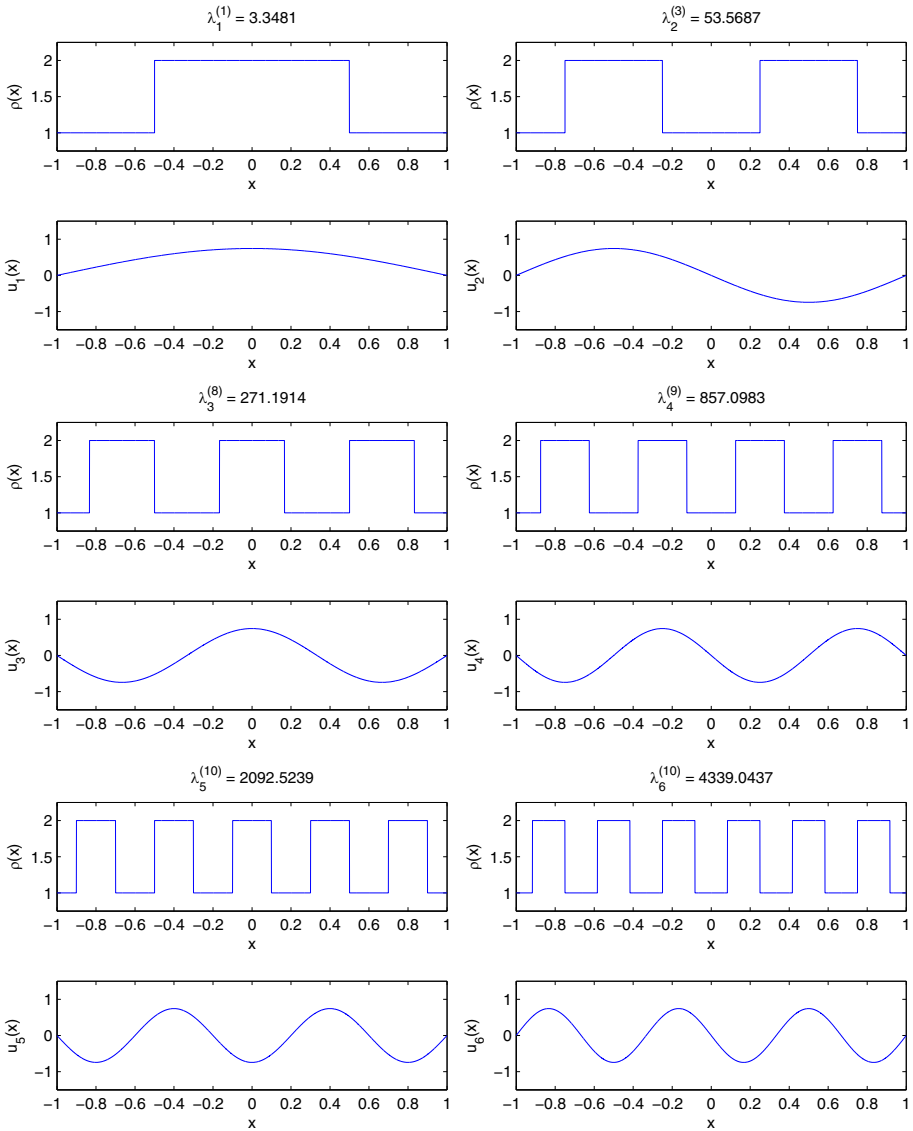


Fig. 3 The optimal density distributions and their corresponding eigenfunctions for the minimization of the first six eigenvalues with hinged boundary conditions

always have larger sizes, whereas for a hinged rod all bumps have the same widths. All the minimization procedures meet the stopping criterion within 10 iterations by the fully sorting algorithm.

5.2 Minimization of λ_k on a Unit Square

Consider the eigenvalue problems (1) and (2) on the unit square $[0, 1] \times [0, 1]$. First, we test the order of accuracy of the forward solver to compute the eigenvalues $\lambda_k, k = 1, \dots, 6$, of

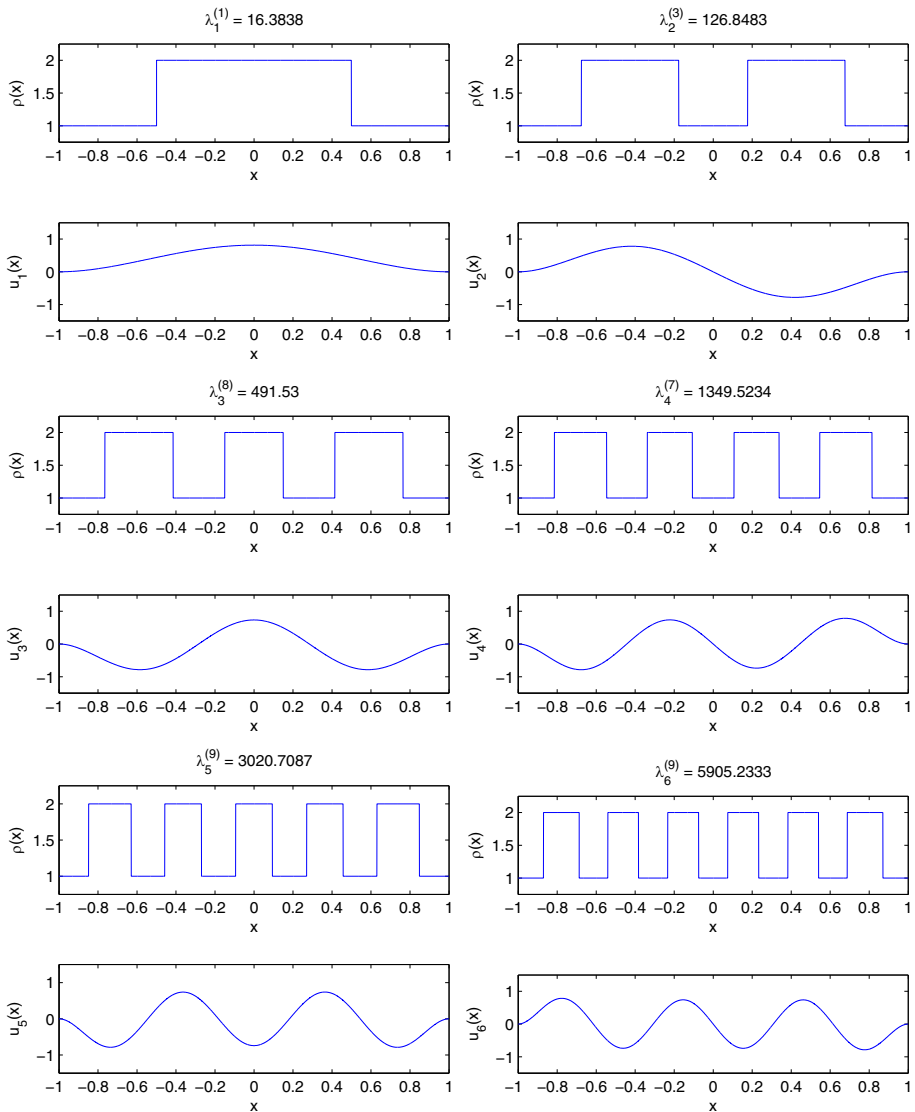


Fig. 4 The optimal density distributions and their corresponding eigenfunctions for the minimization of the first six eigenvalues with clamped boundary conditions

the discretized operator described in Appendix with homogeneous density $\rho(x, y) \equiv 1$. The tested mesh sizes are $h = \frac{1}{50}, \frac{1}{100}, \frac{1}{200}$. The results are shown in Tables 3 and 4. The second order accuracy is clearly observed as the second order central difference scheme is used to approximate the derivatives with either hinged or clamped boundary conditions.

Now we apply the fully sorting algorithm to minimize the eigenvalues of (1) and (2) on the unit square with $\alpha = 1$, and $\beta = 2$. The constraint is set to be $\gamma = 1.5$ which is equivalent to requiring that half of the square is at the high value β of density and the other half is at low value α . We implement the rearrangement algorithm to minimize λ_k for $k = 1, \dots, 5$ on a mesh of 250×250 grid points. Notice that for the homogeneous case,

Table 3 Accuracy test for the first six eigenvalues on $[0, 1] \times [0, 1]$ with hinged boundary conditions

	$h = \frac{1}{50}$	$h = \frac{1}{100}$	$h = \frac{1}{200}$	$\log_2 \left \frac{u_h - u_{\frac{h}{2}}}{\frac{u_{\frac{h}{2}} - u_{\frac{h}{4}}}{2}} \right $
λ_1	389.380069	389.572276	389.620339	2.00
λ_2	2429.785187	2433.865669	2434.886804	2.00
λ_3	2429.785187	2433.865669	2434.886804	2.00
λ_4	6217.793535	6230.081113	6233.156418	2.00
λ_5	9688.485415	9727.778393	9737.624872	2.00
λ_6	9688.485415	9727.778393	9737.624872	2.00

Table 4 Accuracy test for the first six eigenvalues on $[0, 1] \times [0, 1]$ with clamped boundary conditions

	$h = \frac{1}{50}$	$h = \frac{1}{100}$	$h = \frac{1}{200}$	$\log_2 \left \frac{u_h - u_{\frac{h}{2}}}{\frac{u_{\frac{h}{2}} - u_{\frac{h}{4}}}{2}} \right $
λ_1	1289.954088	1293.683924	1294.621142	1.99
λ_2	5348.616237	5377.089561	5384.261203	1.99
λ_3	5348.616237	5377.089561	5384.261203	1.99
λ_4	11612.640048	11686.047874	11704.606299	1.98
λ_5	17104.258221	17260.754751	17300.285961	1.99
λ_6	17270.014283	17425.655941	17464.966689	1.99

only λ_1 and λ_4 are simple among the first five eigenvalues. It is possible that the second and third eigenvalues collide, and the fifth and sixth eigenvalues also collide during the optimization. For the eigenvalue whose multiplicity is greater than 1, it is necessary to search for the optimum based on a combination of neighboring eigenfunctions. Therefore, we need to compare the minimizers obtained by sorting based on a single eigenmode or a combination of multiple ones to guarantee that the global optimum is achieved. In this numerical example, all the minimizers are achieved by sorting based on a single eigenfunction, except that, λ_3 is minimized when λ_2 and λ_3 collide. In addition, we compare the minimizers of hinged and clamped plates in Figs. 5 and 6. For the hinged boundary conditions, similar to the results in one dimension, the optimizer has periodicity in both x - and y -directions. In contrast, the high density compartments are closer to the center of the domain in the optimizers for clamped boundary conditions.

5.3 Minimization of λ_k on an Elongated Rectangle

Consider the eigenvalue problems (1) and (2) with $\alpha = 1$ and $\beta = 2$ on an elongated rectangle $[-r, r] \times [-1, 1]$ where r is some constant greater than 1. Let $r = 5$ so that the length is five times of the width. On such a domain we expect to observe a similar phenomenon to that on a one-dimensional interval when minimizing the first five eigenvalues, under the constraint that half of the rectangle is composed of high density material. The rearrangement algorithm is carried out on a mesh with $h = \frac{1}{50}$ for hinged and clamped boundary conditions. For each eigenmode, the minimizer of λ_k is achieved as a simple eigenvalue, shown in Fig. 7. With hinged boundary conditions, the high density region in the minimizers of λ_k , $k \geq 2$, consists of k compartments of equal size aligned with the long side with periodicity, whereas the

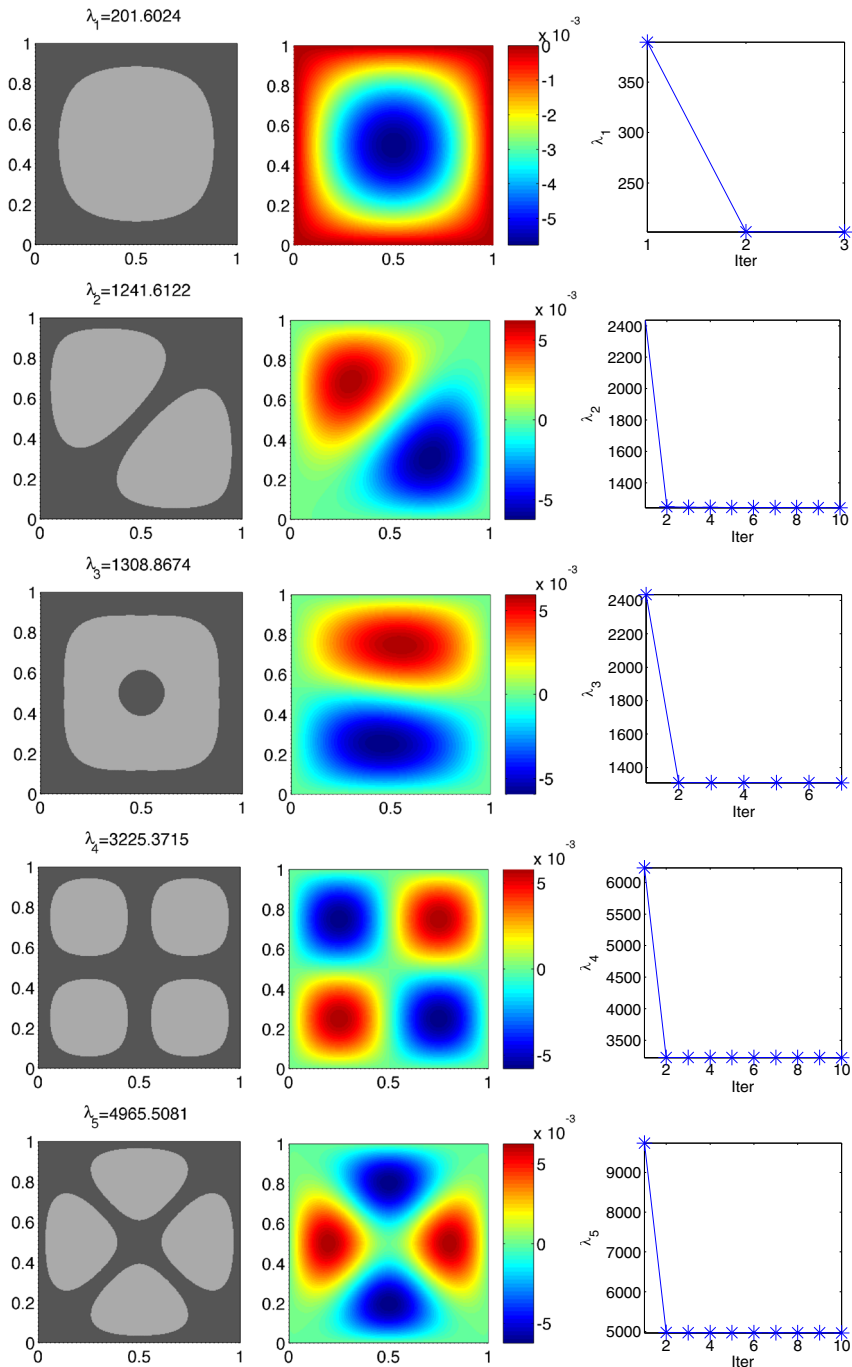


Fig. 5 Minimization of $\lambda_k, k = 1, 2, 3, 4, 5$ on a square domain with hinged boundary conditions. Figures in the *first column* are the optimized density configurations with the *darker color* representing the lower value. Figures in the *second column* are the corresponding eigenfunctions and figures in the *third column* are the convergence history of each eigenvalue. All minimizations converge within 10 iterations

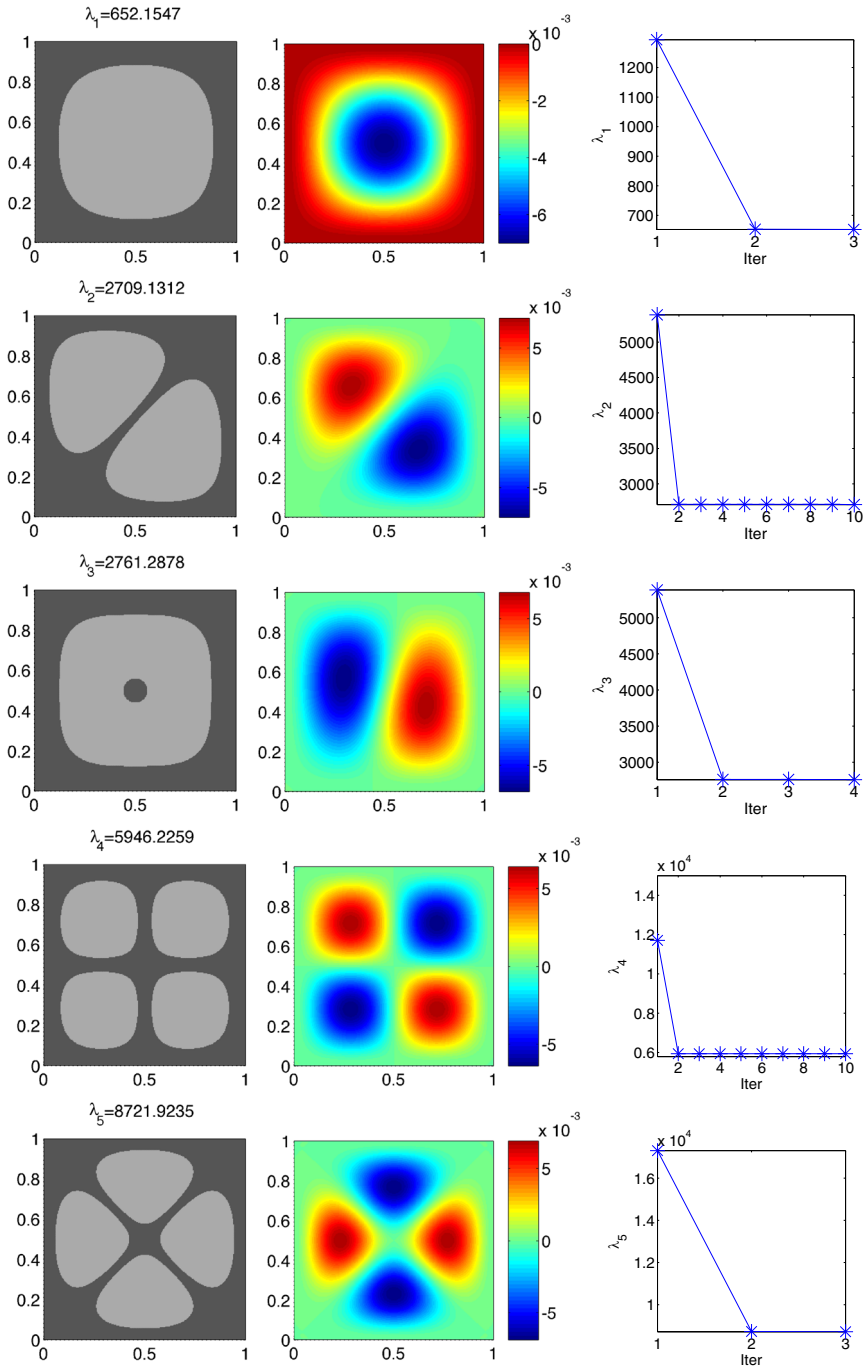


Fig. 6 Minimization of $\lambda_k, k = 1, 2, 3, 4, 5$ on a square domain with clamped boundary conditions. Figures in the *first column* are the optimized density configurations with the *darker color* representing the lower value. Figures in the *second column* are the corresponding eigenfunctions and figures in the *third column* are the convergence history of each eigenvalue. All minimizations converge within 10 iterations

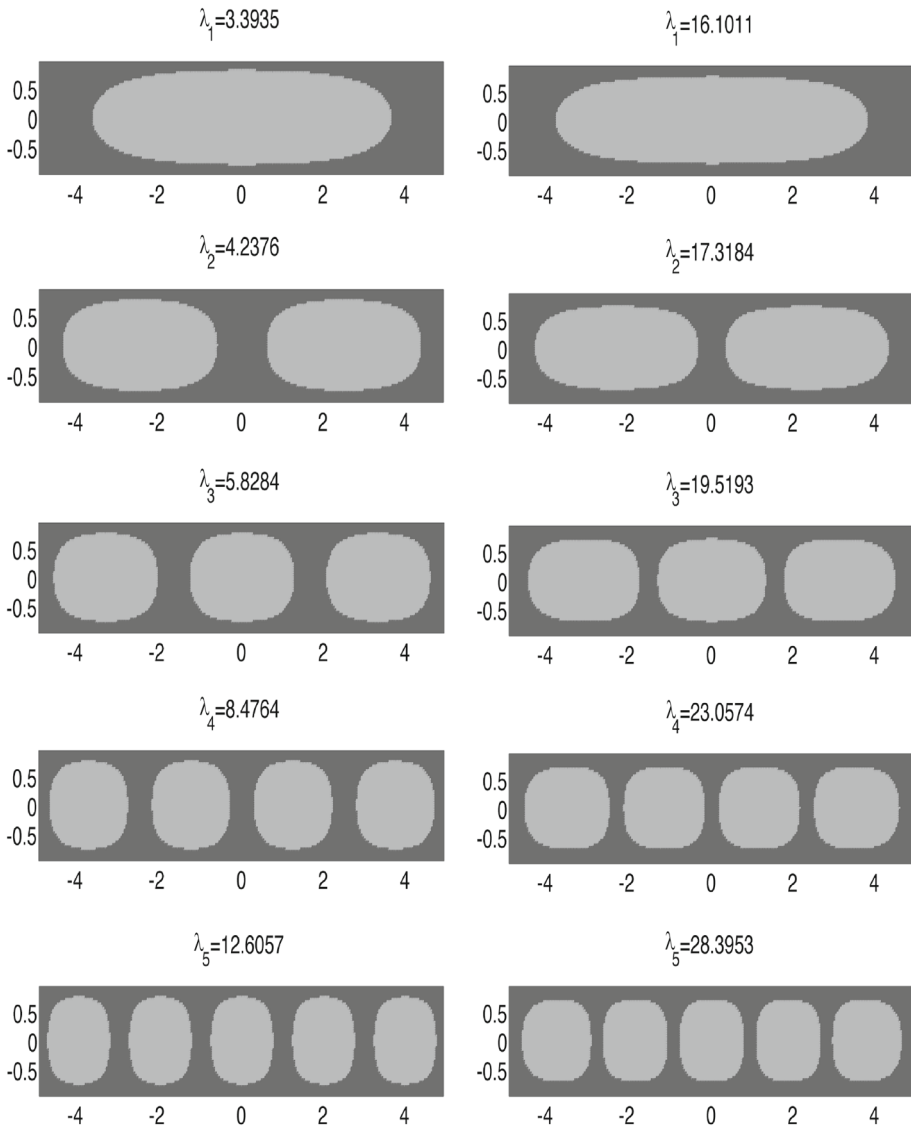


Fig. 7 Optimized density configurations for $\lambda_k, k = 1, 2, 3, 4, 5$, on an elongated rectangle with hinged (*left*) or clamped (*right*) boundary conditions

first and last compartments along the long side show larger sizes when clamped boundary conditions are imposed. This is consistent with what we observed in one-dimensional optimal results.

5.4 Minimization of λ_k on a Unit Disk

Consider the eigenvalue problems (1) and (2) on a unit disk $\{(x, y) : x^2 + y^2 \leq 1\}$ under the constraint that half of the disk consists of the high density material with $\alpha = 1$ and

$\beta = 2$. We perform the rearrangement algorithm to minimize λ_k for $k = 1, \dots, 5$ after converting the equation into polar coordinates on a 350×350 mesh equipped with clamped or simply supported boundary conditions with $\nu = 0.3$. Notice that for the homogeneous density distribution, only the first eigenvalue is simple. The second and third eigenvalues are colliding with each other, so are the fourth and fifth eigenvalues. Therefore, the optimal configuration of the third eigenvalue is achieved when the second and third eigenvalues collide and the fifth eigenvalue is minimized when the fourth and fifth eigenvalues collide. The minimizers of the other eigenvalues are obtained through sorting based on a single eigenfunction. The results are shown in Figs. 8 and 9. When minimizing λ_k with $k \geq 2$, the optimal configurations for clamped boundary conditions have the high density regions closer to the center of the disk, compared with those for simply supported boundary conditions. This is similar to what we observe when the minimization is implemented on a square domain.

5.5 Minimization of λ_k on an Annulus

Consider the eigenvalue problems (1) and (2) on an annular domain $\{(x, y) : r_{in}^2 \leq x^2 + y^2 \leq r_{out}^2\}$, where $r_{in} = 0.4$ and $r_{out} = 1$. The constraint is that half of the annulus consists of the high density material with $\alpha = 1$ and $\beta = 2$. We implement the rearrangement algorithm to minimize λ_k for $k = 1, \dots, 5$ on a 250×250 mesh after converting the equation into polar coordinates for clamped or simply supported boundary conditions with $\nu = 0.3$. On the annular domain with inner radius 0.4, the second and third eigenvalues collide with each other, so do the fourth and fifth eigenvalues for the homogeneous density. Therefore, for λ_3 and λ_5 , the sorting procedure should be implemented in the direction of a combination of neighboring eigenfunctions. As shown in Figs. 10 and 11, the optimal configurations for the second eigenvalue are achieved when it is simple, while the optima are obtained for the third eigenvalue when it collides with the second one. The optimal configurations for the fourth and fifth eigenvalues are obtained in a similar manner. An interesting observation is that for the first eigenvalue, the optimal configuration may not be radially symmetric. This symmetry breaking is analytically studied for harmonic eigenvalue problems on an annular domain [11, 12]. Indeed, a similar phenomenon is observed numerically for the biharmonic eigenvalue problems. On a fixed annular domain, the symmetry of the optimal configuration is related to the composition ratio between two different materials given in the constraint. In Fig. 12, we show the minimization of λ_1 for different proportions of the high density on the annular domain $\{(x, y) : r_{in}^2 \leq x^2 + y^2 \leq r_{out}^2\}$, where $r_{in} = 0.4$ and $r_{out} = 1$. When the proportion is relatively large, the optimal configuration is radially symmetric. The symmetry is gradually lost as the proportion decreases. The threshold for symmetry breaking is between 0.2 and 0.5 as the proportion of the high density region for simply supported boundary conditions, and is between 0.5 and 0.8 for clamped boundary conditions.

When the inner radius is sufficiently small, the principle eigenfunction is not of one sign and the corresponding eigenvalue may have the multiplicity greater than 1 for clamped boundary conditions [14, 44]. We perform the sorting algorithm to minimize $\lambda_k, k = 1, 2$ on the annulus $\{(x, y) : \frac{1}{800^2} \leq x^2 + y^2 \leq 1\}$ under the constraint that half of the annulus consists of the high density material with $\alpha = 1$ and $\beta = 2$. Note that when the density is homogeneous on the clamped punctured disk, the first and second eigenvalues collide, which is different from the case with relatively large inner radius whereas the second and third eigenvalues collide. Therefore, it is possible that the second eigenvalue is minimized when it is colliding with the first one. The mesh is set to be 100×400 after being converted into the polar coordinates (r, θ) . The results by the rearrangement algorithm are shown in Fig. 13. Unlike the minimization in the annulus with $r_{in} = 0.4$, the high density region

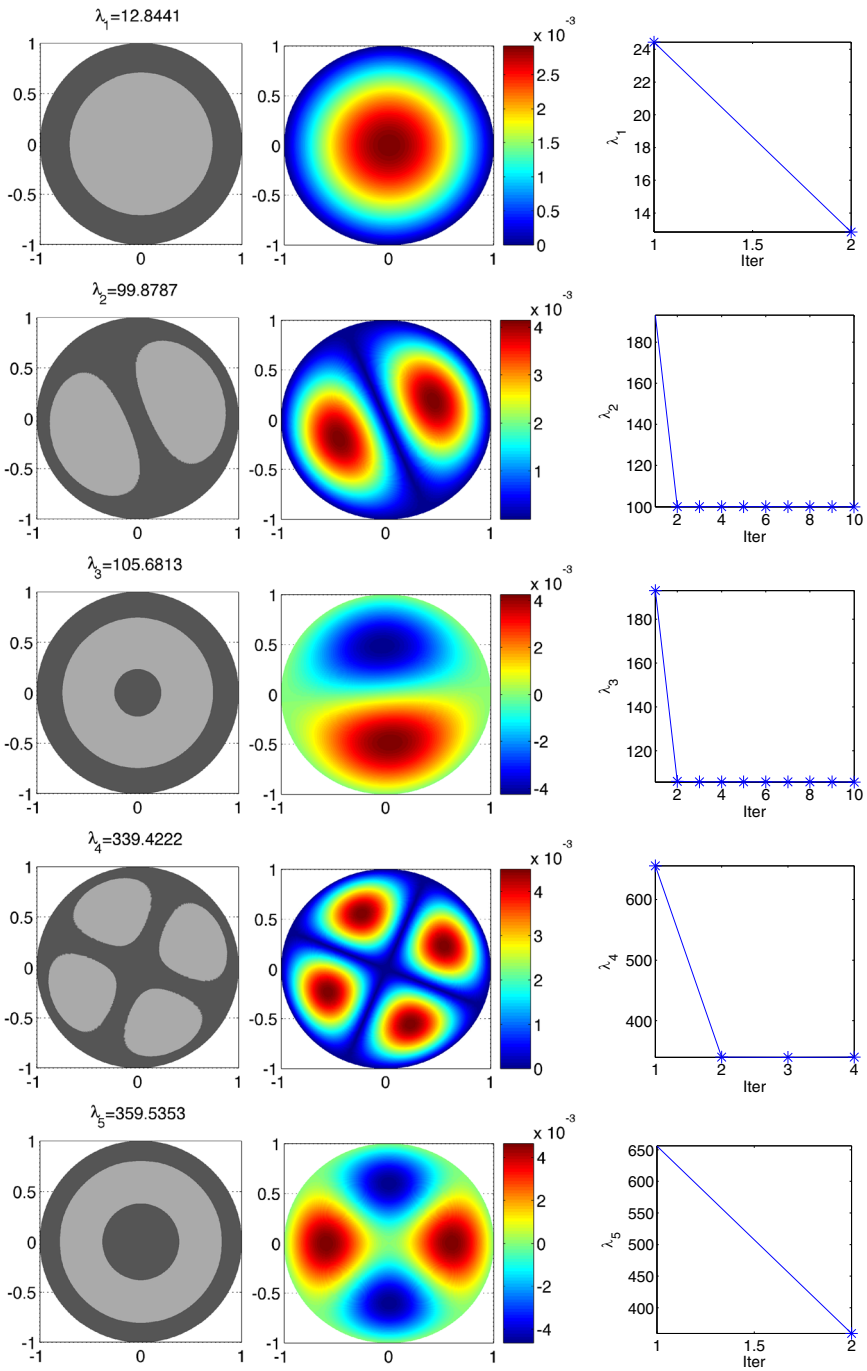


Fig. 8 Minimization of $\lambda_k, k = 1, 2, 3, 4, 5$ on a unit disk with simply supported boundary conditions, $\nu = 0.3$. Figures in the *first column* are the optimized density configurations with the *darker color* representing the lower value. Figures in the *second column* are the corresponding eigenfunctions and figures in the *third column* are the convergence history of each eigenvalue. All minimizations converge within 10 iterations

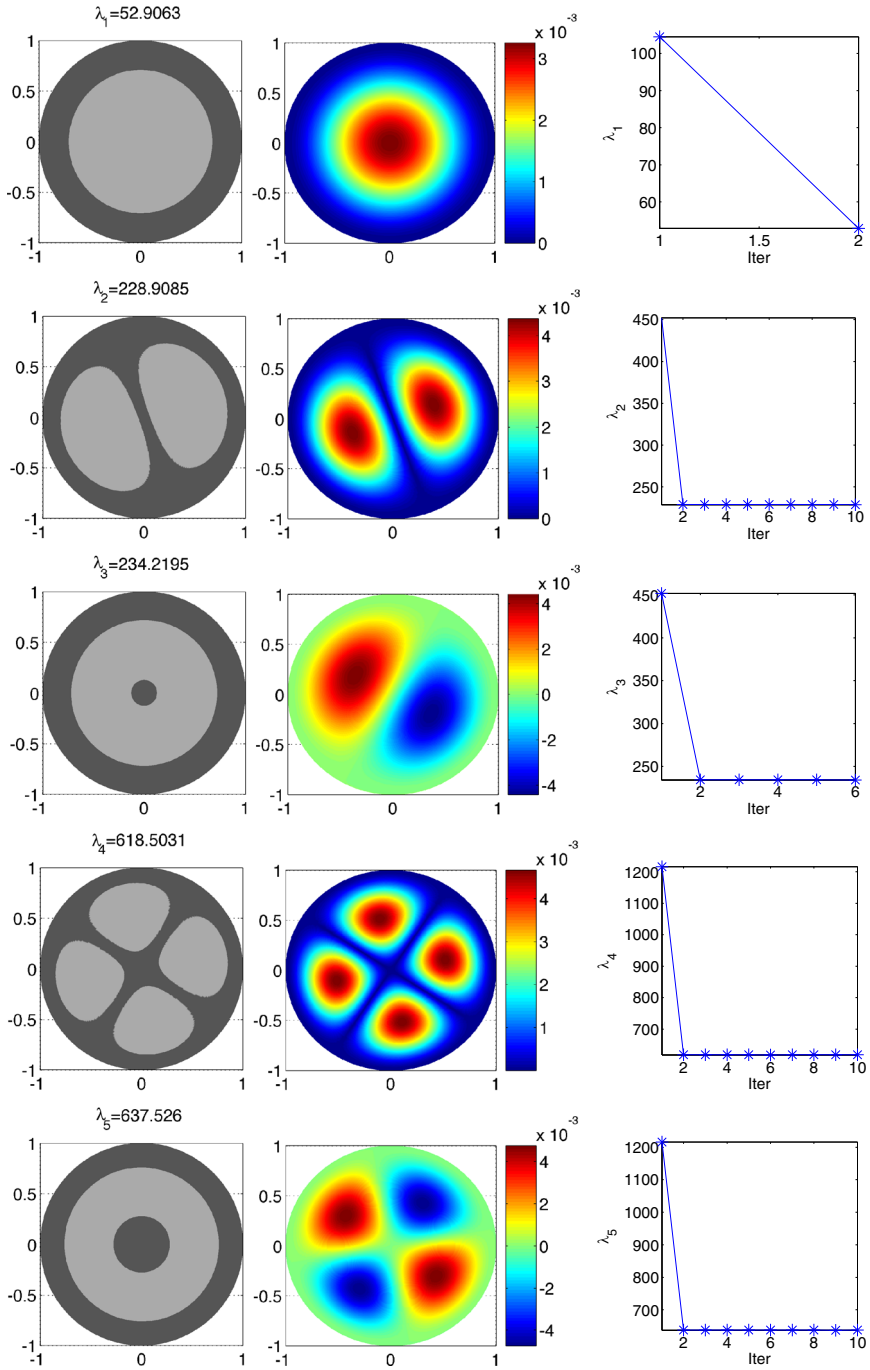


Fig. 9 Minimization of λ_k , $k = 1, 2, 3, 4, 5$ on a unit disk with clamped boundary conditions. Figures in the *first column* are the optimized density configurations with the *darker color* representing the lower value. Figures in the *second column* are the corresponding eigenfunctions and figures in the *third column* are the convergence history of each eigenvalue. All minimizations converge within 10 iterations

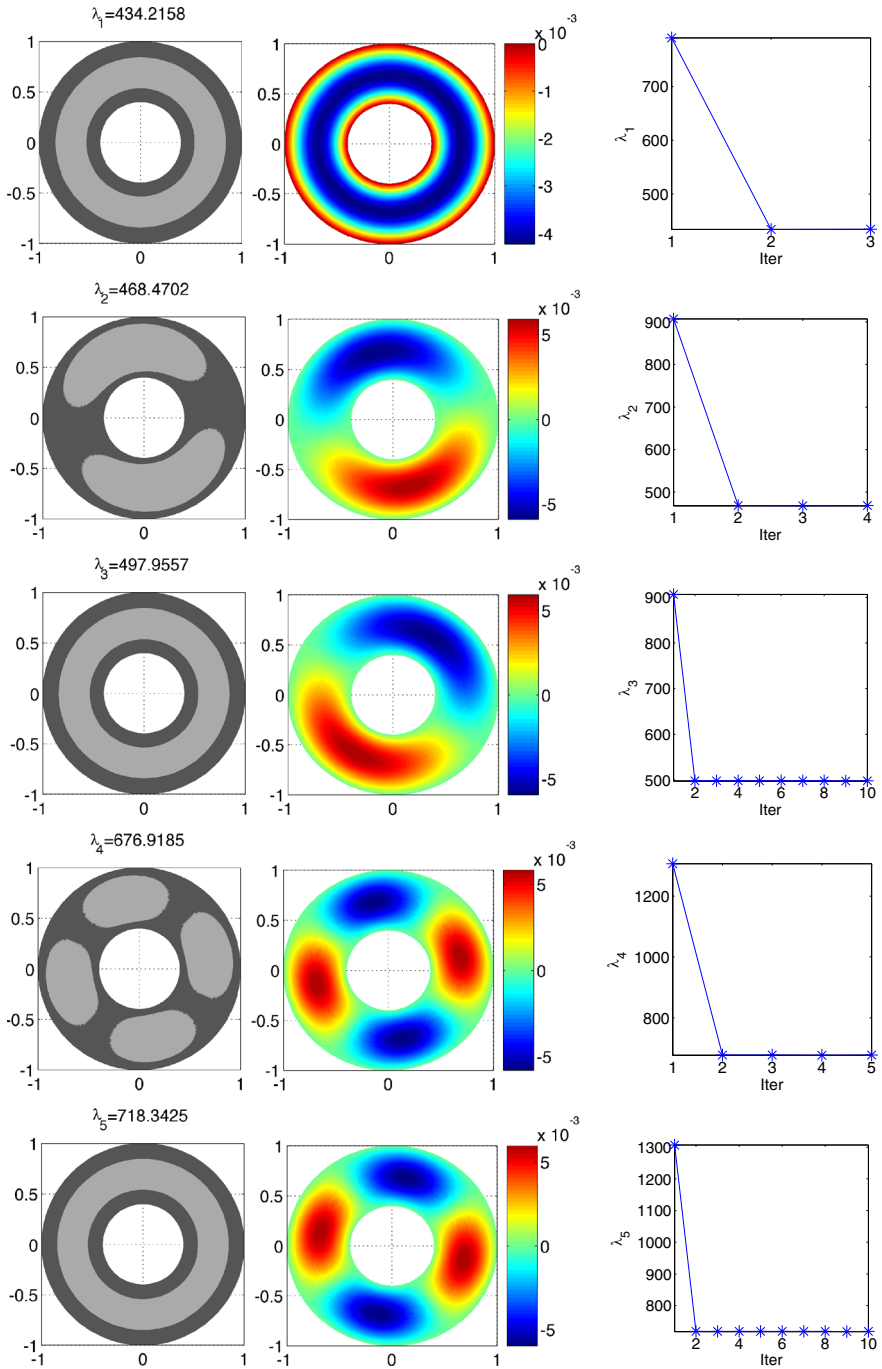


Fig. 10 Minimization of $\lambda_k, k = 1, 2, 3, 4, 5$ on an annulus with $r_{in} = 0.4$ and $r_{out} = 1$ with simply supported boundary conditions, $\nu = 0.3$. Figures in the *first column* are the optimized density configurations with the *darker color* representing the lower value. Figures in the *second column* are the corresponding eigenfunctions and figures in the *third column* are the convergence history of each eigenvalue. All minimizations converge within 10 iterations

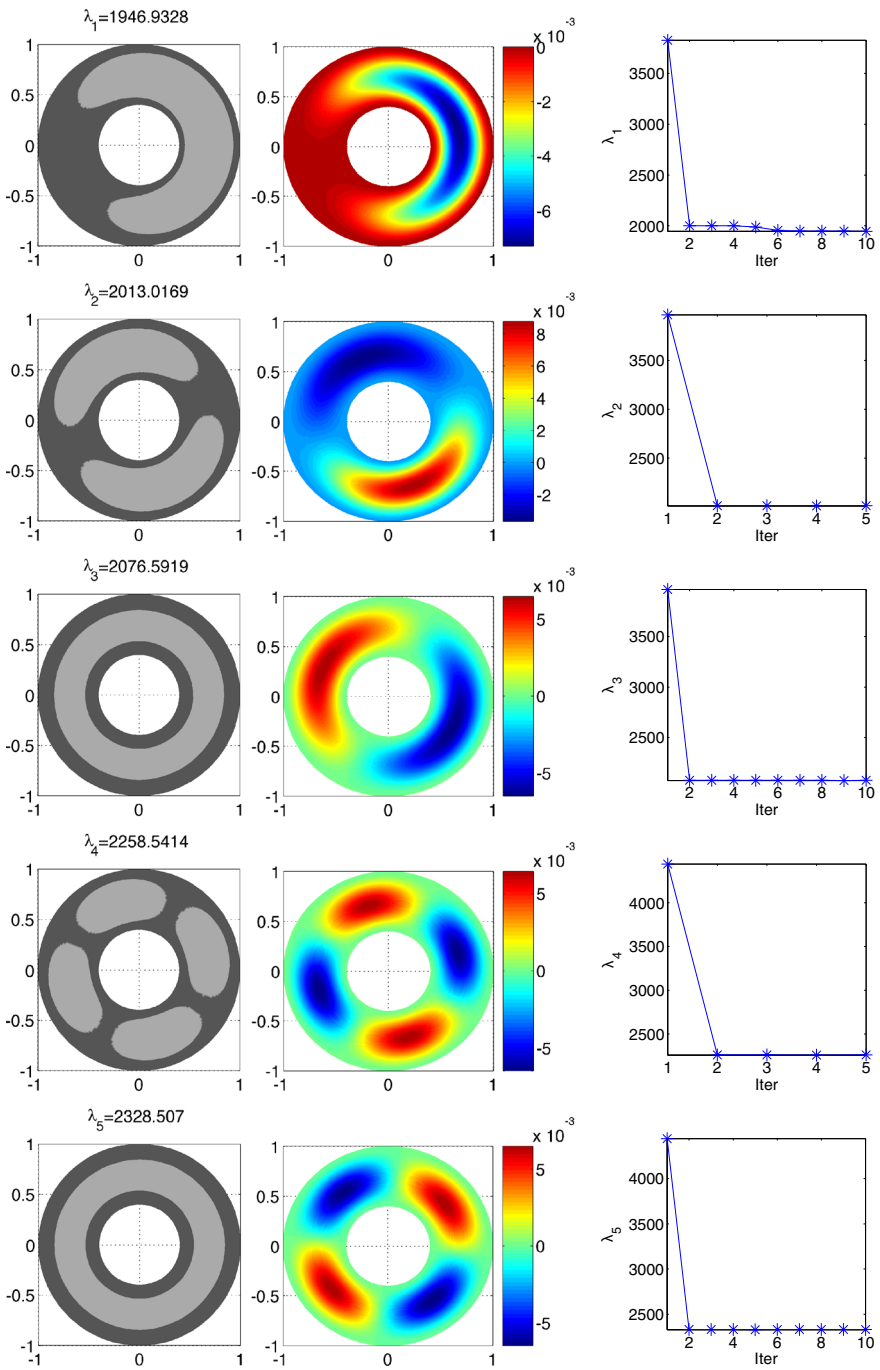


Fig. 11 Minimization of $\lambda_k, k = 1, 2, 3, 4, 5$ on an annulus with $r_{in} = 0.4$ and $r_{out} = 1$ with clamped boundary conditions. Figures in the first column are the optimized density configurations with the *darker color* representing the lower value. Figures in the *second column* are the corresponding eigenfunctions and figures in the *third column* are the convergence history of each eigenvalue. All minimizations converge within 10 iterations

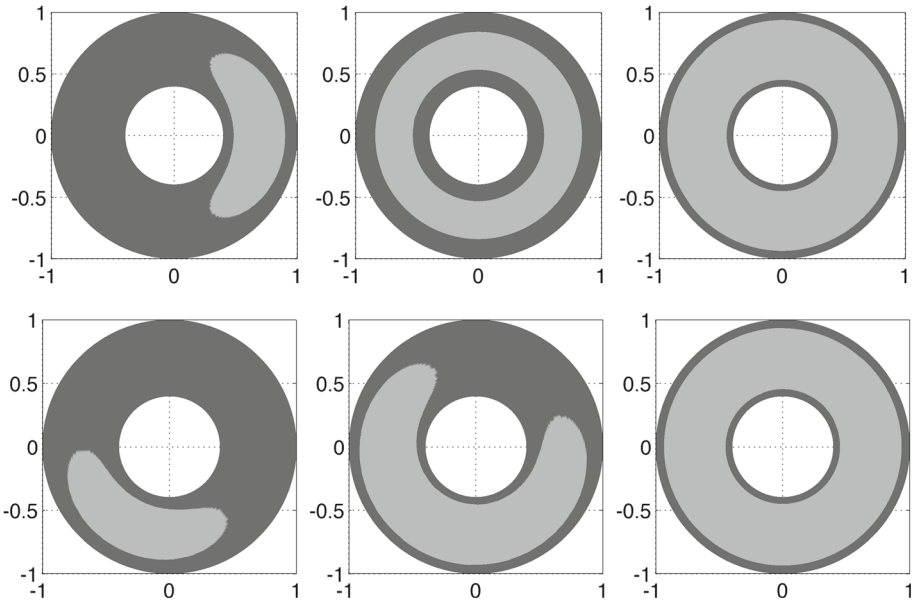


Fig. 12 Optimal density configurations for simply supported (*top*) and clamped (*bottom*) boundary conditions, $\nu = 0.3$, with the proportion of the high density region given as 0.2, 0.5, 0.8 in the constraint, from *left to right*, respectively. The *darker color* represents the lower density. The optimal density is not radially symmetric for the small proportion and becomes symmetric as the proportion increases

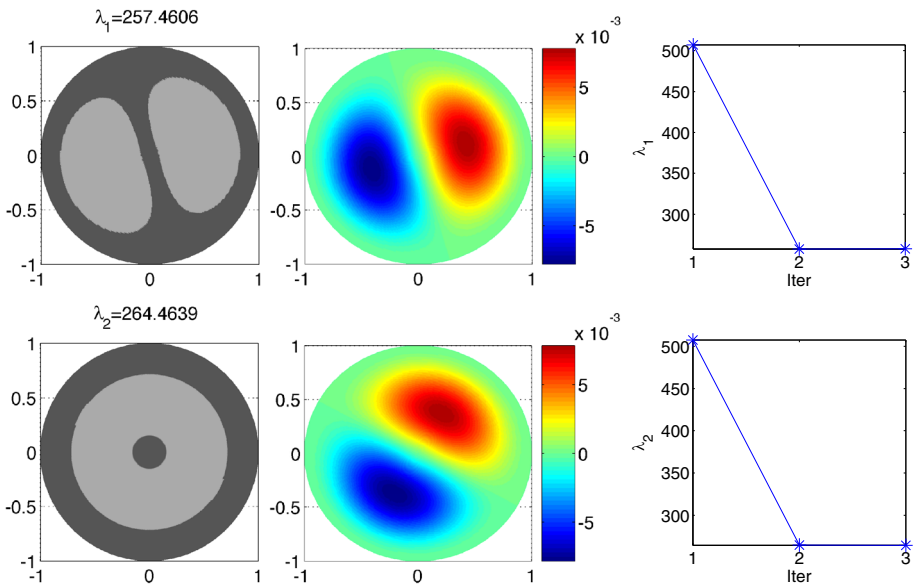


Fig. 13 Minimization of λ_1 and λ_2 on an annulus with $r_{in} = \frac{1}{800}$, $r_{out} = 1$ with clamped boundary conditions. Figures in the *first column* are the optimized density configurations with the *darker color* representing the lower value. Figures in the *second column* are the corresponding eigenfunctions and figures in the *third column* are the convergence history of each eigenvalue. The high density region in the optimized configuration of λ_1 is unconnected and the minimizer of λ_2 is obtained when it collides with λ_1

in the minimizer of the first eigenvalue, obtained as a simple eigenmode, is consisting of two symmetric compartments; the minimizer of the second eigenvalue is obtained when it collides with the first eigenmode and the configuration may exhibit symmetry breaking by perturbing the composition ratio.

6 Discussion

In this paper we are interested in the optimization of weighted biharmonic eigenvalue problems in one- or two-dimensional domains given the constraint that the mass of the materials is fixed. We answer the open question by demonstrating the optimizer of hinged boundary conditions, whose analytic formula has been previously found, is not the optimizer of clamped boundary conditions for eigenvalue $\lambda_k, k \geq 2$, by an asymptotic analysis on a one-dimensional interval. We also numerically solve the minimizer of clamped boundary conditions in one dimension and compare with that of hinged boundary conditions, showing that they are not identical numerically. The analytical formulas of optimizers for clamped boundary conditions require further studies. The rearrangement algorithm is used to minimize eigenvalues on a one-dimensional interval, two-dimensional square, rectangle, unit disk or an annular domain efficiently. This numerical method can be directly applied to other optimization problems, such as buckling equations. When applying this method to more general domains, special treatment may be needed as eigenmodes collide or symmetry breaking occurs.

Appendix 1

In one dimension, for simplicity, we choose $D = [-1, 1]$, and define a uniform grid of points $x_i = -1 + ih$ where h is the mesh size, $0 \leq i \leq N$ and $N = 2/h$. The discretized eigenfunction is denoted by U in the form of a column vector $(U_0, \dots, U_N)^T$. We approximate the fourth order derivative at x_i by the central difference formula

$$U_i'''' \approx \frac{U_{i-2} - 4U_{i-1} + 6U_i - 4U_{i+1} + U_{i+2}}{h^4},$$

for $i = 2, \dots, N - 2$. To approximate the derivatives at x_1 and x_{N-1} , values at ghost points $x_{-1} = -1 - h$ and $x_{N+1} = 1 + h$ are necessary and can be obtained by the given boundary conditions. If clamped boundary conditions are imposed, that is,

$$u(-1) = u(1) = u'(-1) = u'(1) = 0,$$

we choose $U_0 = U_N = 0$ at two end points and $U_{-1} = U_1$ and $U_{N+1} = U_{N-1}$ at two ghost points. Thus

$$U_1'''' \approx \frac{7U_1 - 4U_2 + U_3}{h^4},$$

and

$$U_{N-1}'''' \approx \frac{U_{N-3} - 4U_{N-2} + 7U_{N-1}}{h^4}.$$

The hinged boundary conditions

$$u(-1) = u(1) = u''(-1) = u''(1) = 0$$

lead to $U_0 = U_N = 0$ at the boundaries, $U_{-1} = 2U_0 - U_1$ and $U_{N+1} = 2U_N - U_{N-1}$ at two ghost points. Thus

$$U_1'''' \approx \frac{5U_1 - 4U_2 + U_3}{h^4},$$

and

$$U_{N-1}'''' \approx \frac{U_{N-3} - 4U_{N-2} + 5U_{N-1}}{h^4}.$$

Consequently, the matrix representing the biharmonic operator on $[-1, 1]$ is formed by assigning the coefficients in the approximation formula of U_i'''' to the i -th row.

Appendix 2

In two-dimensional rectangle $D = [-a, a] \times [-b, b]$, define a uniform grid of points $x_{i,j} = (x_{1i}, x_{2j})$ where $x_{1i} = -a + ih_1, x_{2j} = -b + jh_2$ where h_1 and h_2 are mesh sizes in x_1 - and x_2 - directions, respectively. For simplicity, we assume that $h_1 = h_2 = h$. Let $(U_{i,j})_{0 \leq i \leq N, 0 \leq j \leq M}$ be the matrix of the discretized eigenfunction. The second order central difference scheme involving 13-point stencils is used to approximate the biharmonic operator

$$\Delta^2 U_{i,j} \approx \frac{1}{h^4} \begin{bmatrix} & & +U_{i,j+2} & & \\ & +2U_{i-1,j+1} & -8U_{i,j+1} & +2U_{i+1,j+1} & \\ +U_{i-2,j} & -8U_{i-1,j} & +20U_{i,j} & -8U_{i+1,j} & U_{i+2,j} \\ & +2U_{i-1,j-1} & -8U_{i,j-1} & +2U_{i+1,j-1} & \\ & & +U_{i,j-2} & & \end{bmatrix}$$

for $2 \leq i \leq N - 2$, and $2 \leq j \leq M - 2$. With clamped boundary conditions the biharmonic operator along $i = 1$ is approximated by

$$\Delta^2 U_{1,j} \approx \frac{1}{h^4} \begin{bmatrix} +U_{1,j+2} \\ -8U_{1,j+1} & +2U_{2,j+1} \\ +21U_{1,j} & -8U_{2,j} & U_{3,j} \\ -8U_{1,j-1} & +2U_{2,j-1} \\ +U_{1,j-2} \end{bmatrix}, \quad 2 \leq j \leq M - 2,$$

and

$$\Delta^2 U_{1,1} \approx \frac{1}{h^4} \begin{bmatrix} +U_{1,3} \\ -8U_{1,2} & +2U_{2,2} \\ +22U_{1,1} & -8U_{2,1} & U_{3,1} \end{bmatrix}.$$

The approximating formulas along $i = N - 1, j = 1$ or $j = M - 1$ can be derived similarly. All points at the boundaries are taken as zero, $U_{0,j} = U_{N,j} = U_{i,0} = U_{i,M} = 0$. For the hinged boundary conditions, the discretization is almost the same, except the approximations for points near the boundaries ($i = 1$ or $N - 1, j = 1$ or $M - 1$). For example,

$$\Delta^2 U_{1,j} \approx \frac{1}{h^4} \begin{bmatrix} +U_{1,j+2} \\ -8U_{1,j+1} & +2U_{2,j+1} \\ +19U_{1,j} & -8U_{2,j} & U_{3,j} \\ -8U_{1,j-1} & +2U_{2,j-1} \\ +U_{1,j-2} \end{bmatrix}, \quad 2 \leq j \leq M - 2,$$

and

$$\Delta^2 U_{1,1} \approx \frac{1}{h^4} \begin{bmatrix} +U_{1,3} & & & \\ -8U_{1,2} & +2U_{2,2} & & \\ +18U_{1,1} & -8U_{2,1} & U_{3,1} & \end{bmatrix}.$$

The discretization along the other sides can be obtained similarly. Each stencil approximating $\Delta^2 U_{i,j}$ is assigned into a row to form the matrix of the discrete biharmonic operator. Therefore, the size of the matrix to approximate the biharmonic operator on a rectangle is $(N - 1)(M - 1) \times (N - 1)(M - 1)$.

Appendix 3

For the biharmonic eigenvalue problem on a circular or annular domain, we perform the numerical discretization after transforming the problem into the polar coordinates, and the harmonic operator in terms of (r, θ) is

$$\Delta u = \frac{\partial^2 u}{\partial r^2} + \frac{1}{r} \frac{\partial u}{\partial r} + \frac{1}{r^2} \frac{\partial^2 u}{\partial \theta^2}.$$

Assume the domain Ω is a disc with radius one, denoted by $D(0, 1)$. In polar coordinates (r, θ) , the mesh is set to be $r_i = \frac{2i-1}{2N+1}, \theta_j = \frac{2\pi j}{M}, i = 1, 2, \dots, N + 1, j = 1, 2, \dots, M$ to avoid $(0, 0)$. Suppose $U_{(N+1) \times M}$ is the matrix of discretized eigenfunction, then

$$\begin{aligned} \Delta U_{ij} = & \left(\frac{(2N + 1)^2}{4(2i - 1)} + \frac{(2N + 1)^2}{4} \right) U_{i+1,j} + \left(-\frac{(2N + 1)^2}{4(2i - 1)} + \frac{(2N + 1)^2}{4} \right) U_{i-1,j} \\ & + \left(\frac{M(2N + 1)}{2\pi(2i - 1)} \right)^2 (U_{i,j+1} + U_{i,j-1}) - \left(\frac{(2N + 1)^2}{2} + 2 \left(\frac{M(2N + 1)}{2\pi(2i - 1)} \right)^2 \right) U_{ij}. \end{aligned}$$

Near the center, the ghost point $U_{0,j}$ satisfies

$$U_{0,j} = U_{1,j+\frac{M}{2}}.$$

For clamped boundary conditions, we can define ghost points outside $r = 1$ as

$$U_{N+2,j} = U_{N,j}.$$

The simply supported boundary conditions in terms of polar coordinates are written as

$$u = \frac{\partial^2 u}{\partial r^2} + \nu \left(\frac{1}{r^2} \frac{\partial^2 u}{\partial \theta^2} + \frac{1}{r} \frac{\partial u}{\partial r} \right) = 0,$$

where ν is a given constant. Thus we can define

$$U_{N+2,j} = \frac{(\nu h - 2)U_{N,j} + 4U_{N+1,j}}{\nu h + 2}$$

as the ghost points outside $r = 1$. Let L be the discrete operator Δ with clamped or simply supported boundary conditions, then the biharmonic operator is approximated by L^2 after eliminating the last M rows and columns corresponding to the boundary.

The discretization on an annular domain with an inner radius r_{in} and an outer radius r_{out} is similar to the circular case, except that the origin is not included in the domain and therefore the discretized mesh starts at r_{in} and ends at r_{out} in the r -direction. An annulus has both

inner and outer boundaries, and therefore L^2 is obtained by deleting the first and last N rows and columns from the discrete version of the biharmonic operator with clamped or simply supported boundary conditions.

References

1. Anedda, C., Cuccu, F., Porru, G.: Minimization of the first eigenvalue in problems involving the bi-Laplacian. *Revista de Matemática: Teoría y Aplicaciones* **16**(1), 127–136 (2009)
2. Ashbaugh, M.S., Benguria, R.D., et al.: On rayleigh's conjecture for the clamped plate and its generalization to three dimensions. *Duke Math. J.* **78**(1), 1–18 (1995)
3. Banks, D.O.: Bounds for the eigenvalues of some vibrating systems. *Pac. J. Math.* **10**(2), 439–474 (1960)
4. Banks, D.O.: Bounds for the eigenvalues of nonhomogeneous hinged vibrating rods. *J. Math. Mech.* **16**, 949–966 (1967)
5. Beesack, P.R.: Isoperimetric inequalities for the nonhomogeneous clamped rod and plate. *J. Math. Mech.* **8**, 471–482 (1959)
6. Belgacem, F.: *Elliptic Boundary Value Problems with Indefinite Weights, Variational Formulations of the Principal Eigenvalue, and Applications*, vol. 368. CRC Press, Boca Raton (1997)
7. Bendali, A., Fares, M., Tizaoui, A., Tordeux, S.: Matched asymptotic expansions of the eigenvalues of a 3-d boundary-value problem relative to two cavities linked by a hole of small size. *CICP* (2012)
8. Bjørstad, P.E., Tjøstheim, B.P.: High precision solutions of two fourth order eigenvalue problems. *Computing* **63**(2), 97–107 (1999)
9. Brown, B.M., Davies, E.B., Jimack, P.K., Mihajlović, M.D.: On the Accurate Finite Element Solution of a Class of Fourth Order Eigenvalue Problems. arXiv preprint [arXiv:math/9905038](https://arxiv.org/abs/1905.0338) (1999)
10. Buoso, D., Lamberti, P.D.: Shape deformation for vibrating hinged plates. *Math. Methods. Appl. Sci.* **37**(2), 237–244 (2014)
11. Cadeddu, L., Farina, M.A., Porru, G.: Optimization of the principal eigenvalue under mixed boundary condition. *Electron. J. Differ. Equ.* **2014**(154), 1–17 (2014)
12. Chanillo, S., Grieser, D., Imai, M., Kurata, K., Ohnishi, I.: Symmetry breaking and other phenomena in the optimization of eigenvalues for composite membranes. *Commun. Math. Phys.* **214**(2), 315–337 (2000)
13. Chen, W., Diest, K., Kao, C.-Y., Marthaler, D.E., Sweatlock, L.A., Osher, S.: Gradient based optimization methods for metamaterial design. In: Diest, K. (ed.) *Numerical Methods for Metamaterial Design*, pp 175–204. Springer, Netherlands (2013)
14. Coffman, C.V., Duffin, R.J.: On the fundamental eigenfunctions of a clamped punctured disk. *Adv. Appl. Math.* **13**(2), 142–151 (1992)
15. Cox, S.J.: The two phase drum with the deepest bass note. *Jpn. J. Ind. Appl. Math.* **8**(3), 345–355 (1991)
16. Cox, S.J., Dobson, D.C.: Band structure optimization of two-dimensional photonic crystals in H-polarization. *J. Comput. Phys.* **158**(2), 214–224 (2000)
17. Cuccu, F., Emamizadeh, B., Porru, G.: Optimization of the first eigenvalue in problems involving the bi-Laplacian. *Proc. Am. Math. Soc.* **137**(5), 1677–1687 (2009)
18. Cuccu, F., Porru, G.: Maximization of the first eigenvalue in problems involving the bi-Laplacian. *Non-linear Anal. Theory Methods Appl.* **71**(12), e800–e809 (2009)
19. Dobson, D.C., Cox, S.J.: Maximizing band gaps in two-dimensional photonic crystals. *SIAM J. Appl. Math.* **59**(6), 2108–2120 (1999)
20. He, L., Kao, C.-Y., Osher, S.: Incorporating topological derivatives into shape derivatives based level set methods. *J. Comput. Phys.* **225**(1), 891–909 (2007)
21. Henrot, A.: *Extremum Problems for Eigenvalues of Elliptic Operators*. Springer, Berlin (2006)
22. Hintermüller, M., Kao, C.-Y., Laurain, A.: Principal eigenvalue minimization for an elliptic problem with indefinite weight and robin boundary conditions. *Appl. Math. Optim.* **65**(1), 111–146 (2012)
23. Hunter, J.K.: *Asymptotic Analysis and Singular Perturbation Theory*. Department of Mathematics, University of California at Davis (2004)
24. Kao, C.-Y., Lou, Y., Yanagida, E.: Principal eigenvalue for an elliptic problem with indefinite weight on cylindrical domains. *Math. Biosci. Eng.* **5**(2), 315–335 (2008)
25. Kao, C.-Y., Osher, S., Yablonovitch, E.: Maximizing band gaps in two-dimensional photonic crystals by using level set methods. *Appl. Phys. B Lasers Opt.* **81**(2), 235–244 (2005)
26. Kao, C.-Y., Santosa, F.: Maximization of the quality factor of an optical resonator. *Wave Motion* **45**(4), 412–427 (2008)

27. Kao, C.-Y., Shu, S.: Efficient rearrangement algorithms for shape optimization on elliptic eigenvalue problems. *J. Sci. Comput.* **54**(2–3), 492–512 (2013)
28. Karabash, I.M.: Nonlinear eigenvalue problem for optimal resonances in optical cavities. *Math. Model. Nat. Phenom.* **8**(01), 143–155 (2013)
29. Krein, M.G.: On Certain Problems on the Maximum and Minimum of Characteristic Values and on the Lyapunov Zones of Stability. American Mathematical Society Translations. American Mathematical Society (1955)
30. Lehoucq, R.B., Sorensen, D.C., Yang, C.: ARPACK Users Guide: Solution of Large-Scale Eigenvalue Problems with Implicitly Restarted Arnoldi Methods, vol. 6. SIAM, Philadelphia, PA (1998)
31. Lin, J., Santosa, F.: Resonances of a finite one-dimensional photonic crystal with a defect. *SIAM J. Appl. Math.* **73**(2), 1002–1019 (2013)
32. Lou, Y., Yanagida, E.: Minimization of the principal eigenvalue for an elliptic boundary value problem with indefinite weight, and applications to population dynamics. *Jpn. J. Ind. Appl. Math.* **23**(3), 275–292 (2006)
33. Maksimović, M., Manfred Hammer, E.W.C., van Groesen, B.: Coupled optical defect microcavities in one-dimensional photonic crystals and quasi-normal modes. *Opt. Eng.* **47**(11), 114601–114601 (2008)
34. Men, H., Lee, K.Y.K., Freund, R.M., Peraire, J., Johnson, S.G.: Robust topology optimization of three-dimensional photonic-crystal band-gap structures. *Opt. Express* **22**(19), 22632–22648 (2014)
35. Men, H., Nguyen, N.-C., Freund, R.M., Lim, K.-M., Parrilo, P.A., Peraire, J.: Design of photonic crystals with multiple and combined band gaps. *Phys. Rev. E* **83**(4), 046703 (2011)
36. Mohammadi, S.A., Bahrami, F.: Extremal principal eigenvalue of the bi-Laplacian operator. *Appl. Math. Model.* **40**(3), 2291–2300 (2016)
37. Mohr, E.: Über die rayleighsche vermutung: Unter allen platten von gegebener fläche und konstanter dichte und elastizität hat die kreisförmige den tiefsten grundton. *Annali di matematica pura ed applicata* **104**(1), 85–122 (1975)
38. Nadirashvili, N.S.: Rayleigh’s conjecture on the principal frequency of the clamped plate. *Arch. Ration. Mech. Anal.* **129**(1), 1–10 (1995)
39. Osher, S.J., Santosa, F.: Level set methods for optimization problems involving geometry and constraints: I. Frequencies of a two-density inhomogeneous drum. *J. Comput. Phys.* **171**(1), 272–288 (2001)
40. Osting, B.: Bragg structure and the first spectral gap. *Appl. Math. Lett.* **25**(11), 1926–1930 (2012)
41. Rayleigh, J.W.S.: *The Theory of Sound*, vol. 1. McMillan, New York (1945)
42. Schwarz, B.: Some results on the frequencies of nonhomogeneous rods. *J. Math. Anal. Appl.* **5**(2), 169–175 (1962)
43. Sigmund, O., Hougaard, K.: Geometric properties of optimal photonic crystals. *Phys. Rev. Lett.* **100**(15), 153904 (2008)
44. Sweers, G.: When is the first eigenfunction for the clamped plate equation of fixed sign. *Electron. J. Differ. Equ. Conf.* **6**, 285–296 (2001)
45. Szegő, G.: On membranes and plates. *Proc. Natl. Acad. Sci. USA* **36**(3), 210 (1950)
46. Talenti, G.: On the first eigenvalue of the clamped plate. *Ann. Mat.* **129**(1), 265–280 (1981)
47. Wayne, A.: Inequalities and inversions of order. *Scr. Math.* **12**(2), 164–169 (1946)
48. Yolcu, S.Y., Yolcu, T.: Estimates on the eigenvalues of the clamped plate problem on domains in Euclidean spaces. *J. Math. Phys.* **54**(4), 043515 (2013)